

Cyclooxygenase inhibition attenuates brain angiogenesis and independently decreases mouse survival under hypoxia

Drew R. Seeger  | Svetlana A. Golovko | Bryon D. Grove | Mikhail Y. Golovko 

Department of Biomedical Sciences,
University of North Dakota, Grand Forks,
ND, USA

Correspondence

Mikhail Y. Golovko, Department of
Biomedical Sciences, School of Medicine
and Health Sciences, University of North
Dakota, 1301 N. Columbia Rd., Grand Forks,
ND 58202-9037, USA.
Email: mikhail.golovko@med.und.edu

Funding information

National Institute of General Medical
Sciences, Grant/Award Number:
5P30GM103329; National Institute
of Neurological Disorders and Stroke,
Grant/Award Number: 5R21NS109856,
P20GM113123 and U54GM128729

Abstract

Although cyclooxygenase (COX) role in cancer angiogenesis has been studied, little is known about its role in brain angiogenicity. In the present study, we chronically infused mice with ketorolac, a non-specific COX inhibitor that does not cross the blood–brain barrier (BBB), under normoxia or 50% isobaric hypoxia (10% O₂ by volume). Ketorolac increased mortality rate under hypoxia in a dose-dependent manner. Using in vivo multiphoton microscopy, we demonstrated that chronic COX inhibition completely attenuated brain angiogenic response to hypoxia. Alterations in a number of angiogenic factors that were reported to be COX-dependent in other models were assayed at 24-hr and 10-day hypoxia. Intriguingly, hypoxia-inducible factor 1 was unaffected under COX inhibition, and vascular endothelial growth factor receptor type 2 (VEGFR2) and C-X-C chemokine receptor type 4 (CXCR4) were significantly but slightly decreased. However, a number of mitogen-activated protein kinases (MAPKs) were significantly reduced upon COX inhibition. We conclude that additional, angiogenic factor-independent mechanism might contribute to COX role in brain angiogenicity, probably including mitogenic COX effect on endothelium. Our data indicate that COX activity is critical for systemic adaptation to chronic hypoxia, and BBB COX is essential for hypoxia-induced brain angiogenicity. These data also indicate a potential risk for using COX inhibitors under hypoxia conditions in clinics. Further studies are required to elucidate a complete mechanism for brain long-term angiogenesis regulation through COX activity.

KEYWORDS

angiogenesis, brain, cyclooxygenase, hypoxia, non-steroidal anti-inflammatory drugs, prostaglandins

Abbreviations: 6-ketoF_{1α}, 6-keto prostaglandin F_{1α}; BBB, blood–brain barrier; COX, cyclooxygenase; CXCR4, C-X-C chemokine receptor type 4; ELISA, enzyme-linked immunosorbent assay; ERK 1/2, extracellular signal-regulated kinase; FGF, fibroblast growth factor; FGFR1, fibroblast growth factor receptor 1; HIF, hypoxia-inducible factor; HMECs, human microvascular endothelial cells; i.p., intraperitoneal; MAPK, mitogen-activated protein kinases; MRM, multiple reaction monitoring; MS, mass spectrometry; NSAID, non-steroidal anti-inflammatory drugs; p38, stress-activated protein kinase-2; PG, prostaglandin; PGD₂, prostaglandin D₂; PGE₂, prostaglandin E₂; PGF_{2α}, prostaglandin F_{2α}; PPAR, peroxisome proliferator-activated receptor; RRID, Research Resource Identifier; s.c., subcutaneous; SAPK/JNK, stress-activated protein kinase/Jun-amino-terminal kinase; SDF-1, stromal-derived factor 1; TxB₂, thromboxanes; UPLC, ultra-high-pressure liquid chromatography; VEGF, vascular endothelial growth factor; VEGFR2, vascular endothelial growth factor receptor 2; Δ(12)-PGJ₂, delta-12-prostaglandin J₂.

This is an open access article under the terms of the Creative Commons Attribution-NonCommercial-NoDerivs License, which permits use and distribution in any medium, provided the original work is properly cited, the use is non-commercial and no modifications or adaptations are made.

© 2021 The Authors. *Journal of Neurochemistry* published by John Wiley & Sons Ltd on behalf of International Society for Neurochemistry.



1 | INTRODUCTION

Physiological brain angiogenesis, often named angioplasticity (LaManna, 2018) to differentiate from pathological angiogenesis, has a critical role in long-term physiological adaptation to low-energy conditions including chronic hypoxia (Benderro & LaManna, 2014; Ndubuizu et al., 2010). Using complementary quantification methods, it is documented that 7-day and longer exposure to moderate (9%–11% of O₂) chronic hypoxia almost doubles brain capillary density and branching points in a rodent brain (Benderro & LaManna, 2014; Cramer et al., 2019; Ward et al., 2007). Further angiogenesis is quenched after ~14 days' exposure to hypoxia (Harb et al., 2013; Harik et al., 1996), probably because of compensatory restoration of O₂ supply. Brain vascular plasticity is also important for long-term adaptation to increased energy consumption during learning and training. In fact, a positive correlation between cognition and cerebral perfusion has been demonstrated in several studies (Ding et al., 2006; Morland et al., 2017; Wightman et al., 2015). Alternatively, impaired brain vascular plasticity may contribute to declined memory and learning (Licht et al., 2011), and neurodegeneration including age-related dementia (Tarkowski et al., 2002). In addition, hypoxia-induced angiogenesis is an important pathogenic factor for tumor development including brain tumors (Amin & Katerina, 1996; Kleihues et al., 2002). Given the importance of adult brain angiogenesis for physiological and pathophysiological plasticity, a deeper mechanistic understanding of brain angiogenesis has both basic neuroscience and clinical/translational importance to therapeutic vessel modulation for pathological processes where aberrant angiogenesis is involved.

A number of mechanisms contribute to hypoxia-induced angiogenesis. Hypoxia activates local cellular production of pro-angiogenic growth factors such as vascular endothelial growth factors (VEGF), fibroblast growth factors (FGF), angiopoietins, chemokines including stromal-derived factor 1 (SDF-1), and corresponding receptors (Jun et al., 2020; Nakatsu et al., 2003; Pichiule & LaManna, 2002; Salcedo et al., 2003; Simon et al., 2008; Ward et al., 2007) through a hypoxia-inducible factor (HIF-1/2)-dependent mechanism (Dvorak, 2005; Madrigal-Martínez et al., 2018; Sharp & Bernaudin, 2004). Importantly, mitogen-activated protein kinases (MAPK) including extracellular signal-regulated kinase (ERK), stress-activated protein kinases (SAPK)/c-Jun NH₂-terminal kinase (JNK), and stress-activated protein kinase-2 (p38) are required to transduce the signals generated by growth factors, cytokines, and other stress factors to stimulate endothelial cell migrations and proliferation as critical steps of angiogenesis (Matsumoto et al., 1999; Mavria et al., 2006; Medhora et al., 2008; Rousseau et al., 1997).

In addition, based on the observation that brain COX-2 expression is induced under prolonged moderate hypoxia (Benderro & LaManna, 2014; LaManna et al., 2006), the role for COX in brain hypoxia-induced angiogenesis has been proposed. This hypothesis is further supported by the direct effect of COX products on a number of angiogenic factors (Fukuda et al., 2003; Jurek et al., 2004; Tsujii et al., 1998; Tuncer & Banerjee, 2015; Zhao et al., 2012) (Finetti

et al., 2008; Kang et al., 2007; Katori et al., 1998; Leahy et al., 2000; Salcedo et al., 2003), as well as indirect COX effect on angiogenesis through MAPK pathway (Cho & Choe, 2020; Riquelme et al., 2015). However, to the best of our knowledge, no direct lines of evidence have been provided to support COX role in the adult brain angioplasticity, although COX role in tumor-induced angiogenesis is well documented (Katoh et al., 2010; Li et al., 2002; Wang et al., 2014). Many tumors have increased COX-2 expression (Chen et al., 2019; Ferrario et al., 2002; Jalota et al., 2018; Wang & Dubois, 2010), and treatment with non-steroidal anti-inflammatory drugs (NSAID) decreases tumor angiogenesis (Jalota et al., 2018; Leahy et al., 2000). However, it is unclear if COX inhibition with NSAID directly suppresses angiogenesis, or this is the result of tumor growth suppression through anti-mitotic (Lee et al., 2007; Sharma et al., 2011) or anti-inflammatory effects of NSAID. Despite a significant progress in elucidating the role for COX in the tumor-related angiogenesis, it is still unclear if similar mechanisms apply to normal tissue including brain. In addition, many previous studies were performed using implanted sponge or matrigel (Katoh et al., 2010; Salcedo et al., 2003; Zhang & Daaka, 2011), on cell cultures of endothelial (Zhao et al., 2012) or retinal cells (Yanni et al., 2010), corneal micropocket assay after surgical intervention (Verheul et al., 1999), and utilizing exogenous prostaglandins (Yanni et al., 2010; Zhang & Daaka, 2011; Zhao et al., 2012), making it difficult to translate these results to brain physiological angioplasticity.

In the current study, we addressed, for the first time, the effect of blood–brain barrier (BBB) COX inhibition on hypoxia-induced brain angiogenesis in mice using an *in vivo* imaging assay. Our data indicate that COX activity is critical for systemic adaptation to chronic hypoxia, and BBB COX is essential for hypoxia-induced brain angioplasticity that affects angiogenesis partially through VEGFR and C-X-C chemokine receptor type 4 (CXCR4) expression and MAPK pathway, but independently from HIF/bFGF/angiopoietin signaling. Because of the small magnitude of VEGFR and CXCR changes upon COX inhibition under hypoxia, additional mechanisms involving MAPK pathway might have a bigger role in COX-dependent brain angioplasticity. Further studies are required to elucidate a complete mechanism for brain long-term angiogenesis regulation through COX activity.

2 | METHODS

2.1 | Animals

This study was conducted in accordance with the National Institutes of Health Guidelines for the Care and Use of Laboratory Animals and under an animal protocol approved by the University of North Dakota IACUC (Protocol 0708-1c), and in compliance with Animal Research: Reporting *In Vivo* Experiments (ARRIVE) guidelines (Percie du Sert et al., 2020). Ninety-four male C57BL/6 mice (Jackson Laboratory, 2–3 months old) were given standard laboratory chow and water *ad libitum*. Animals were randomly assigned to experimental groups

using simple randomization procedure. Specifically, animals in each cage were coded with tail marks using a marker, and cages were marked with numbers. These data were entered into an Excel spreadsheet that generated an animal identification number in the format cage number/animal number. To meet the requirements of simple randomization (Suresh, 2011), before treatment, the researcher moved animals from housing cages to treatment cages, alternately assigning to control or experimental group independently from the tail code. A red color tail mark was added to code a cage number, and the animal identification number was matched to the experimental group on the Excel spreadsheet. This protocol allowed for a random non-bias animal assignment to experimental groups (Suresh, 2011). All experiments were performed during daylight time. The sample size (four to six animals per group) was determined using power analysis (Statmate2, Graphpad, San Diego), with expected 40 to 30% difference between groups (based on previous studies), 20% RSD, $\alpha = 0.05$, and power = 0.8, except for PG analysis where the sample size ($n = 3$) was based on our previous study of COX inhibition upon ketorolac treatment (Seeger et al., 2020). The methods used for data collection and analysis, including automatic software-based image processing and chromatogram integrations, are unbiased and did not require blinding to the experimental groups; however, the researcher was blind to the experimental groups during western blot image integration. The study was not pre-registered. No animals were excluded from analysis. The measures to minimize animal suffering after treatment/during experiments were approved by the University of North Dakota IACUC (Protocol 0708-1c) and included wetting eyes with ophthalmic ointment to prevent drying during the surgery and imaging, 1.0% lidocaine (topical) for additional pain control, placing animals after surgery in a temperature-controlled environment with the external temperature 26°C maintained using a heated pad, and animals were checked daily for signs of bleeding, inflammation, infection (redness, appearance of infection, swelling), distress/sickness. To collect animals for basal PG analysis, mice were killed with isoflurane (2%–3%) followed by focused microwave

irradiation (2.8 kW, 1.35 s, Cober Electronics, Inc, Norwalk, CT) to heat denature enzymes in situ (Brose et al., 2011, 2016). To collect animals for protein and biochemical analysis, mice were killed with isoflurane (2%–3%) followed by decapitation.

2.2 | Experimental design

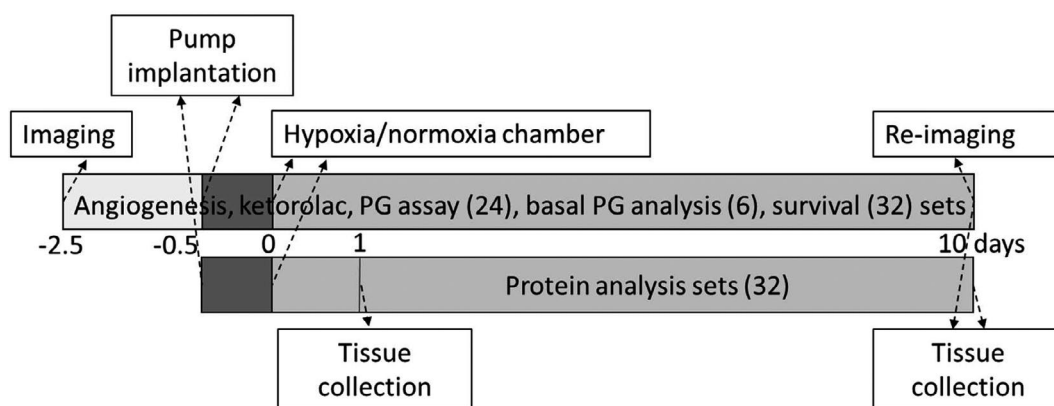
We used two sets of mice, with hypoxia- and normoxia-exposed groups within each set (Scheme 1). One set was used for transcranial vasculature imaging with multiphoton microscopy followed by tissue collection for ketorolac brain and plasma concentration, and prostanoid analysis. Another set was used for brain protein analysis.

Each group was treated with saline (vehicle control) or different doses of ketorolac using implanted osmotic pumps. Pumps were implanted 12 hr before placing animals under hypoxia or normoxia atmosphere to allow ketorolac to reach steady-state concentration and to allow animal recovery after implantation surgery. It took 6 to 12 hr for ketorolac to reach steady-state plasma concentration as was determined using LC-MS assay (data not shown).

For in vivo imaging, mice were subjected to skull thinning and fluorescent dye injection, and transcranial vasculature was visualized using multiphoton microscopy 2 days before pump implantation (2.5 days before placing animals under normoxia or hypoxia environment (Scheme 1)) to allow recovery after the surgery. Transcranial vasculature was re-imaged 10 days after exposure to hypoxia or normoxia.

2.3 | Transcranial vasculature imaging with multiphoton microscopy

Mice were anesthetized with ketamine (100 mg/kg) and xylazine (10 mg/kg) and fixed in a heated stereotaxic surgery device. The skull was exposed by a midline incision and remaining fascia



SCHEME 1 Experimental design. Each set of mice was randomly divided into two groups: one for hypoxia (10% O₂) and another for normoxia (20% O₂) treatment. All mice within these sets were implanted with osmotic pumps filled with either saline (control) or different doses of ketorolac to inhibit COX activity. First set was used for transcranial vascular imaging and tissue collection for ketorolac assay and prostanoid quantification, and the second set was used for tissue collection for specific proteins quantification. Numbers in parentheses indicate the total number of animals used per group



removed by scraping with a scalpel. For *in vivo* imaging, a thinned cranial window approximately 3 mm in diameter was made over the somatosensory cortex using a high-speed drill. The skull was thinned until soft (30 μm) as previously described (Harb et al., 2013; Yang et al., 2010). Conjugated TRITC-dextran 500,000 Daltons (25 mg/ml in saline, 200 μl , Millipore-Sigma, St. Louis; MO cat.no. 52194) was injected via tail vein to visualize brain vasculature. After exposure to normoxia or hypoxia, transcranial vasculature was re-imaged using the same methods as described. A light re-thinning of the skull was required because of regrowth. However, conjugated FITC-dextran 2,000,000 Daltons (25 mg/ml in saline, 200 μl) (Millipore-Sigma, St. Louis; MO cat.no. FD2000S) was injected through the tail vein to reduce background noise from previously injected TRITC-dextran.

Immediately after fluorescent probe injection, the mouse was imaged using an Olympus FV1000 MPE Basic multiphoton microscope equipped with a Mai Tai (Spectra-Physics, Santa Clara, USA) Ti:Sapphire laser set to 810nm and 1.5%–2% output, an XLPlan N 25x (NA 1.04, 2 mm WD) water immersion lens, and a 495–540 nm and 575–630 nm emission filters for FITC and TRITC, respectively. An imaging area located away from large vessels was chosen via epifluorescent visualization through the eyepiece and then once the top of the pia layer was located, optical sections were collected to a depth of 300 μm using a 2 μm Z step size. The scan rate was 8 s/frame with two Kalman filter cycles and the scanning area was 509 $\mu\text{m} \times 509 \mu\text{m}$ (640 \times 640 pixels). Laser power was kept under 2% to prevent thermal damage to superior vessels. The 3D Z-stack image was analyzed using a TubeAnalyst macro (IRB Barcelona) available for Fiji (Image J) software (Schindelin et al., 2012) with blood vessel segmentation and network analysis. The total number of junctions, branches, and total vessel length were normalized to the image volume. After imaging, the surgical area was closed with 7mm skin clips (Kent scientific). The area was covered with antibiotic ointment and the mice were allowed to recover on a heated pad before being returned to their home cages.

2.4 | Osmotic pump implantation

Two days following vasculature imaging, osmotic pumps (Alzet, Cupertino, CA cat.no. 2002) were implanted subcutaneously according to the manufacturer's instructions under isoflurane anesthesia (1%–3%). Pumps were filled with either saline or ketorolac (Cayman Chemical Company, Ann Arbor; MI cat.no. 70690) dissolved in saline. Pumping rate was 0.5 $\mu\text{l}/\text{hour}$. The ketorolac concentration was adjusted to the animal weight to achieve 0.64, 1.28, and 6.4 mg/kg/hour, and was 0.0255, 0.0512, and 0.256 mg/ μl , respectively, for a 20-g mouse.

2.5 | Hypoxia and normoxia treatment

Twelve hours following osmotic pump implantation, mice were randomly separated into two groups using a simple randomization

procedure as described above. One group was exposed to hypoxia, while another to normoxia. Mice in the hypoxia group were placed into a Biospherix hypoxia chamber (Biospherix oxycycler A84) and exposed to isobaric hypoxia by automatic mixing of oxygen with nitrogen to achieve 10% oxygen (by volume) in the chamber. Mice in the normoxia group were placed in the chamber under 20% oxygen. After a 10-day hypoxia or normoxia, transcranial vasculature was re-imaged as described above. Following the second imaging, mice were killed, and plasma and brain were collected with brains immediately frozen in liquid nitrogen. Samples were analyzed for drug concentration and prostaglandin levels to confirm osmotic pump function. A separate hypoxia and normoxia groups of mice with implanted pumps were used to analyze brain proteins after 24-hr and 10-day hypoxia or normoxia treatment.

2.6 | Ketorolac and prostaglandin analysis

To confirm osmotic pump performance, plasma and brains were extracted for ketorolac assay. Plasma was collected by heart puncture and placed in heparinized tubes on ice. Plasma (20 μl) or brains (20 mg) were extracted in 80 μl of methanol containing 2.5 ng PGE₂D₉ (Cayman Chemical, Ann Arbor, MI, USA cat.no. 10581) as an internal standard (Brose et al., 2013b; Seeger et al., 2020). Following centrifugation, 10 μl of supernatant was injected into the ultra-high-pressure liquid chromatography – mass spectrometry (UPLC-MS) system for analysis as previously described (Seeger et al., 2020). Briefly, we used a high-resolution accurate mass MS (G2S, Waters) operated in positive electrospray ionization mode. Quantification was performed against PGE₂D₉ after separation on Waters Acquity UPLC with water/acetonitrile gradient and formic acid as modifier on Waters ACUITY UPLC HSS T3 column (1.8 μm , 100 Å pore diameter, 2.1 \times 150mm, Waters, Milford, MA) with an ACUITY UPLC HSS T3 pre-column (1.8 μm , 100 Å pore diameter, 2.1 \times 5mm, Waters) at a temperature of 55°C (Seeger et al., 2020). Selected ion monitoring was used for ketorolac ($m/z = 256.0974 \pm 0.02$ Da, retention time 3.00 min) and PGE₂D₉ ($m/z = 326.2680 \pm 0.02$ Da, retention time 3.25 min) quantification (Seeger et al., 2020). No noticeable matrix effect was found for ketorolac and PGE₂D₉ under these conditions, and the relative response curve built against PGE₂D₉ was linear from 10 pg to 100 ng of ketorolac on column.

For prostanoid analysis, whole brain was removed, flash frozen in liquid nitrogen, and then pulverized into a homogenous powder under liquid nitrogen conditions. Following pulverization, prostanoids were extracted using an acetone liquid/liquid extraction method as previously described (Brose et al., 2011). Briefly, brains were homogenized in acetone/saline (2:1) with 2.5 ng PGE₂D₉ (Cayman Chemical, Ann Arbor, MI cat.no. 10581) as an internal standard, washed with hexane, and extracted with chloroform, dried under a stream of nitrogen, in 20 μl of acetonitrile:water (1:1) and injected into the UPLC-MS system for analysis as previously described (Brose & Golovko, 2013). Briefly, UPLC separation was performed on Waters ACUITY UPLC HSS T3 column (1.8 μm , 100 Å pore diameter, 2.1 \times 150mm, Waters,

Milford, MA) with an ACUITY UPLC HSS T3 pre-column (1.8 μ M, 100 Å pore diameter, 2.1 \times 5mm, Waters) at a temperature of 55°C. A gradient of water with 0.1% formic acid/acetonitrile with 0.1% formic acid was used to resolve prostanoids (Brose & Golovko, 2013). Prostanoids were analyzed using a triple quadrupole mass spectrometer (Xevo TQ-S, Waters) with electrospray ionization operated in negative ion mode. MS conditions and MS/MS mass transitions were as previously described (Brose & Golovko, 2013). PGE₂D₉ was used as an internal standard for quantification.

2.7 | Western blot

Tissue was homogenized in RIPA buffer (50mM Tris, pH 7.4, 150mM NaCl, 1 mM Vanadate, 10 mM NaF, 1 mM EDTA, 1% Triton, 0.5% deoxycholate) with protease inhibitor cocktail set III (Millipore-Sigma, Burlington, MA cat.no. 539134) by sonication. Total protein concentration was measured using the Pierce BCA protein assay kit with a bovine serum albumin standard according to the manufacturer's instructions (Thermo-Fisher Scientific, Waltham, MA cat.no. 23225). The samples were then diluted with 2x Laemmli sample buffer (Bio-Rad, cat.no. 161-0737) containing 5% β -mercaptoethanol and heated to 80°C for 5 min. Proteins were separated by SDS-PAGE (Biorad, TGX FastCast Kit, 7.5% cat.no.1610171) and transferred onto polyvinylidene difluoride (PVDF) membrane (Thermo-Fisher Scientific, cat.no. 88518) by wet tank electroblotting. Following transfer, the membrane was blocked with 3% BSA in TBS-T (50 mM Tris, 150 mM NaCl, 0.1% Tween-20) for 1 hr at room temperature (~20–22 °C). Blocking buffer was replaced with primary antibody in TBS-T with 1% BSA and incubated overnight at 4°C. The following antibodies were used for western blotting: mouse monoclonal β -Actin 1:2,500 (R&D Systems, Minneapolis, MN, cat.no. MAB8929), rabbit polyclonal COX-2 1:500 (Abcam, Cambridge, MA, cat.no. ab15191, RRID: AB_2085144), rabbit polyclonal COX-1 1:200 (Cayman, cat.no. 160109, RRID: AB_10077936), rabbit polyclonal phospho-FGFR1 1:500 (ThermoFisher, cat.no. PA5-104789, RRID: AB_2816262), rabbit monoclonal Angiopoietin-2 1:2000 (ThermoFisher, cat.no. MA5-32759, RRID: AB_2810036), rabbit monoclonal VEGFR2 1:1,000 (ThermoFisher, cat.no. MA5-15157, RRID: AB_10986085), rat monoclonal CXCR4 1:500 (R&D Systems, cat.no. MAB21651, RRID: AB_2261636), rabbit polyclonal p38 1:1,000 (Cell Signaling Technology, Danvers, MA, cat.no. 9212, RRID: AB_330713), rabbit polyclonal phospho-p38 1:1,000 (Cell Signaling Technology, cat.no. 9211, RRID: AB_331641), rabbit monoclonal ERK1/2 1:1,000 (Cell Signaling Technology, cat.no. 4695, RRID: AB_390779), rabbit monoclonal phospho-ERK1/2 1:1,000 (Cell Signaling Technology, cat.no. 4370, RRID: AB_2315112), and rabbit polyclonal SAPK/JNK 1:1,000 (Cell Signaling Technology, cat.no. 9252, RRID: AB_2250373). Following incubation with primary antibody, the membrane was rinsed and then incubated with the appropriate secondary antibody: goat polyclonal anti-mouse HRP 1:5,000 (R&D Systems, cat.no. HAF007, RRID: AB_357234), goat polyclonal anti-rat HRP 1:5,000 (R&D Systems, cat.no. HAF005, RRID: AB_1512258), or goat

polyclonal anti-rabbit HRP 1:2,500 (KPL, cat.no. 474-1516, RRID: AB_2857917). The membrane was then visualized with SuperSignal West Pico Plus chemiluminescent substrate (ThermoFisher Scientific cat.no. 34580) and imaged using an Azure Biosystems c600 imaging system (Dublin, CA). Optical density was quantified using Adobe Photoshop 2020 and normalized to actin.

2.8 | ELISA

Mouse VEGF DuoSet ELISA (R&D Systems, cat.no. DY493), mouse FGF basic DuoSet ELISA (R&D Systems, cat.no. DY3139), and human/mouse Total HIF-1 alpha IC ELISA (R&D Systems, cat.no. DY1935) were used in accordance with the manufacturer's instructions. Pulverized tissue was dissolved in Lysis Buffer #11 (50 mM Tris pH 7.4, 200 mM NaCl, 10% (w/v) glycerol, 3 mM EDTA, 1 mM MgCl₂, 20 mM β -glycerophosphate, 25 mM NaF, 1% Triton X-100) with protease inhibitor cocktail set III (Millipore-Sigma, Burlington, MA cat.no. 539134) by sonication. Total protein concentration was measured using the Pierce BCA protein assay kit with a bovine serum albumin standard according to the manufacturer's instructions (Thermo-Fisher Scientific, Waltham, MA cat.no. 23225). ELISA was performed in a 96-well plate format and the optical density was determined at 450nm and corrected at 540nm using a FlexStation 3 microplate reader (Molecular Devices). The standard curve was generated using GraphPad Prism 8 (Graphpad, San Diego) with a four parameter logistic (4-PL) curve fit. Results were interpolated and normalized to protein concentration.

2.9 | Statistical analysis

Statistical Analysis were performed using GraphPad Prism 8 (Graphpad, San Diego; CA). Statistical significance was determined by either one-way ANOVA or two-tailed Students *t* test. Values were considered significant when *p* < .05 and are expressed as mean \pm SD. Because for small sample sizes normality tests have little power, no assessment of the normality of data was carried out. No test for outliers was conducted.

3 | RESULTS

3.1 | Survival under hypoxia

To adjust a treatment dose, mice were continuously infused with three different doses of ketorolac and exposed to normoxia or moderate isobaric 50% hypoxia (10% oxygen by volume in ambient air). These experiments also allowed us to test the effect of COX inhibition on systemic adaptation to hypoxia. As shown on Figure 1, ketorolac significantly increased mortality rate under hypoxia as compared to normoxia in a dose-dependent manner. Continuous infusion of low doses of ketorolac (0.64 and 1.28 mg kg⁻¹ h⁻¹,

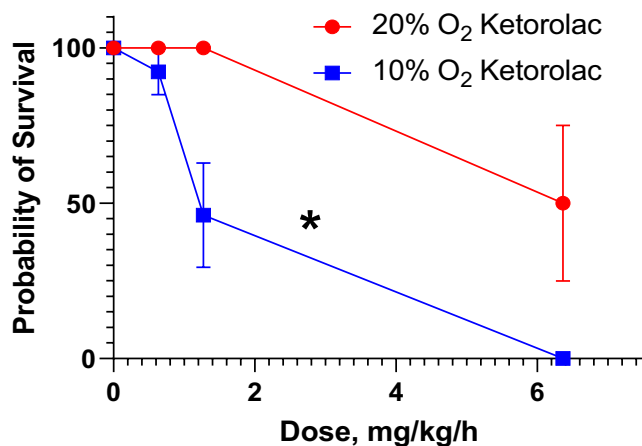


FIGURE 1 Ketorolac significantly increased mortality rate under hypoxia. Mice were treated with ketorolac using implanted osmotic pumps. (*) indicate a significant increase in mortality rate upon exposure to 10-day isobaric hypoxia in a dose-dependent manner ($p = .004$ using Long-rank (Mantel-Cox) test, n (number of animals) = four or five per treatment dose). Deaths occurred between 9 and 10 days of hypoxia

subcutaneously with micro-osmotic pump) did not affect survival under normoxia, but caused 10% and 50% mortality, respectively, under hypoxia on days 9 and 10. A higher dose ($6.4 \text{ mg kg}^{-1} \text{ h}^{-1}$) increased mortality rate to 100% under hypoxia, and 50% under normoxia between 9 and 10 days of treatment. These data indicate that COX activity is essential for systemic adaptation to hypoxia. We used a lower $0.64 \text{ mg kg}^{-1} \text{ h}^{-1}$ infusion rate in further experiments because animals had a higher survival rate while still significantly affected under hypoxia.

3.2 | Ketorolac tissue concentrations and prostanoid synthesis inhibition

At the selected $0.64 \text{ mg kg}^{-1} \text{ h}^{-1}$ infusion rate, ketorolac plasma concentration was 41.09 ± 4.59 ($n = 4$) $\mu\text{mole/L}$ in hypoxic and 48.74 ± 7.59 ($n = 4$) $\mu\text{mole/L}$ in normoxic animals (Table 1). Brain concentration was 0.57 ± 0.08 $\mu\text{mole/kg}$ ($n = 4$) in hypoxic (1.4% from plasma) and 0.72 ± 0.14 ($n = 4$) $\mu\text{mole/kg}$ in normoxic animals (1.5% from plasma) (Table 1), indicating that ketorolac concentration was unaffected by hypoxia, and increased mortality rate is not related to drug concentration alterations under hypoxia. These data

also confirm our previous observation that ketorolac does not cross BBB (Seeger et al., 2020) because ketorolac found in the brain is accounted for by the drug presented in the brain residue blood (Seeger et al., 2020). These results indicate that ketorolac effect on brain angiogenesis is mediated through the components of BBB.

At this plasma concentration, ketorolac inhibited ~80% of brain prostanoid production caused by animal decapitation (a model for brain global hypoxia/ischemia (Brose et al., 2013a, 2016; Farias et al., 2008; Golovko & Murphy, 2008a, 2008b)) (Figure 2). A 10-fold increase in ketorolac infusion rate ($6.4 \text{ mg kg}^{-1} \text{ h}^{-1}$) resulted in a proportional increase in plasma ketorolac concentration to $530.72 \pm 100.84 \mu\text{M}$ ($n = 5$). At similar concentrations challenged in our previous study (Seeger et al., 2020), ketorolac did not cross BBB and completely inhibited brain prostanoid induction under hypoxia/ischemia (Seeger et al., 2020) that was also confirmed in the present study (data not shown). Under complete prostanoid production conditions, all animals died under hypoxia but half of the animals survived under normoxia (Figure 1), indicating that systemic adaptation to hypoxia depends upon prostanoid production in the body.

3.3 | COX levels and PG production under hypoxia and ketorolac treatment

At 10-day hypoxia, we did not detect alterations in the basal brain prostanoid levels measured after in situ enzyme inactivation with microwave irradiation in hypoxic compared to normoxic tissue (Figure 2). However, all prostanoids measured without inhibiting post-mortem prostanoid production, when tissue was extracted without heat denaturing by microwave irradiation, were significantly and uniformly increased 1.6- to 1.7-fold in hypoxic brain (Figure 2). These prostanoids represent inducible by ischemia-hypoxia pool (Brose et al., 2013a, 2016; Farias et al., 2008; Golovko & Murphy, 2008a, 2008b). Thus, the increased inducible PG levels might be related to increased COX activity under hypoxia, while unchanged basal level might indicate a relatively small pool of hypoxia-sensitive prostanoids that is not detected with our method. Similarly, consistent with previous results (Seeger et al., 2020), we did not detect alteration in basal prostanoid pool upon ketorolac treatment (data not shown) but found a significant inhibition in inducible prostanoid pool (Figure 2).

Consistent with inducible prostanoid level increase under hypoxia, brain COX-2 protein levels were significantly 1.4-fold and

TABLE 1 Ketorolac concentration and brain/plasma distribution after 10 days of chronic subcutaneous infusion with osmotic pumps

Normoxia			Hypoxia		
Plasma, μM	Brain, $\mu\text{mole/kg}$	% In brain versus plasma	Plasma, μM	Brain, $\mu\text{mole/kg}$	% In brain versus plasma
41.09 ± 4.59	0.57 ± 0.08	$1.49 \pm 0.17\%$	48.74 ± 7.59	0.72 ± 0.14	$1.57 \pm 0.25\%$

Note: Plasma and brain samples were collected after a 10-day ketorolac continuous infusion with implanted osmotic pumps (s.c.) at $0.62 \text{ mg kg}^{-1} \text{ h}^{-1}$ under isobaric normoxia (20% O₂) or hypoxia (10% O₂). Ketorolac concentration was analyzed using an LC-MS method against internal standard after protein precipitation with methanol. Values are mean \pm standard deviation, n (number of animals) = 4.

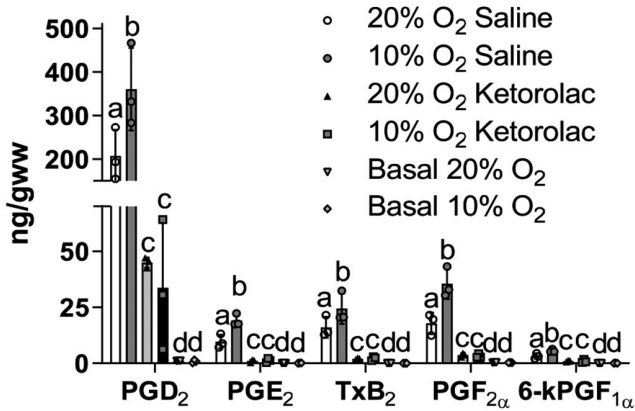


FIGURE 2 Brain prostanoid changes upon 10-day hypoxia and ketorolac treatment. Mice were continuously infused with ketorolac ($0.62 \text{ mg kg}^{-1} \text{ h}^{-1}$) or saline using implanted osmotic pumps under isobaric normoxia ($20\% \text{ O}_2$) or hypoxia ($10\% \text{ O}_2$) for 10 days. Brain prostanoids were quantified without de-activating COX activity during tissue collection and represent inducible prostanoid pool. Basal levels in hypoxic and normoxic brains (last two sets) were determined in brain tissue subjected to head-focused microwave irradiation to heat denature COX activity and represent a true basal PG concentration under normoxia and hypoxia. Prostanoids were analyzed using LC-MS after tissue liquid-liquid extraction. Values are mean \pm standard deviation and individual values (n (number of animals) = 3). Values that do not share the same letter are statistically different ($p < .05$, one-way ANOVA with Tukey's post hoc test)

2.0-fold increased at 10-day hypoxia with and without ketorolac, respectively, as compared to normoxic control brain (Figure 3). Brain COX-2 up-regulation under hypoxia is in line with previous studies (Benderro & LaManna, 2014) and indicate a possible mechanism for increased PG production upon stimulation. However, COX-1 was

unaffected under hypoxia or ketorolac treatment (Figure 3), indicating the predominant role for COX-2 isoenzyme in adaptation to hypoxia. Also, uniformly increased PG levels further indicate that COX-2 activity itself is responsible for increased brain PG production under hypoxia rather than regulation of downstream prostanoid synthases, although other mechanisms such as arachidonic acid availability upon PLA_2 activation or post-translational modifications (Alexanian & Sorokin, 2017) can complement increased COX-2 levels to increase PG production under hypoxia.

Treatment with ketorolac at $0.64 \text{ mg kg}^{-1} \text{ h}^{-1}$ significantly induced brain COX-2 at 24-hr normoxia or hypoxia (~ 1.7 -fold compared to saline-infused normoxic and hypoxic animals, Figure 3), and at 10-day hypoxia (2.0-fold, 1.3-fold, and 1.4-fold increase compared to saline normoxic, saline hypoxic, and ketorolac normoxic animals, respectively). However, similar to hypoxia, ketorolac did not alter COX-1 protein levels (Figure 3). These data indicate a compensatory mechanism for COX-2 inhibition through COX-2 protein increase.

3.4 | Ketorolac effect on hypoxia-induced brain angiogenesis

To quantify brain angiogenesis, we imaged transcranial vasculature using a multiphoton microscopy (Harb et al., 2013; Masamoto et al., 2013). The advantage of this approach is that it allows for a minimally invasive re-imaging of the same brain vascular area in the same animal before and after treatment to accurately quantify changes in brain microvasculature. This significantly eliminates the contribution of individual differences in vascular density between animals, and reduces bias of the assay. Ten-day hypoxia significantly induced the number of branches, junctions, and triple points (~ 1.4 -fold compared to normoxia), total vessel length and volume,

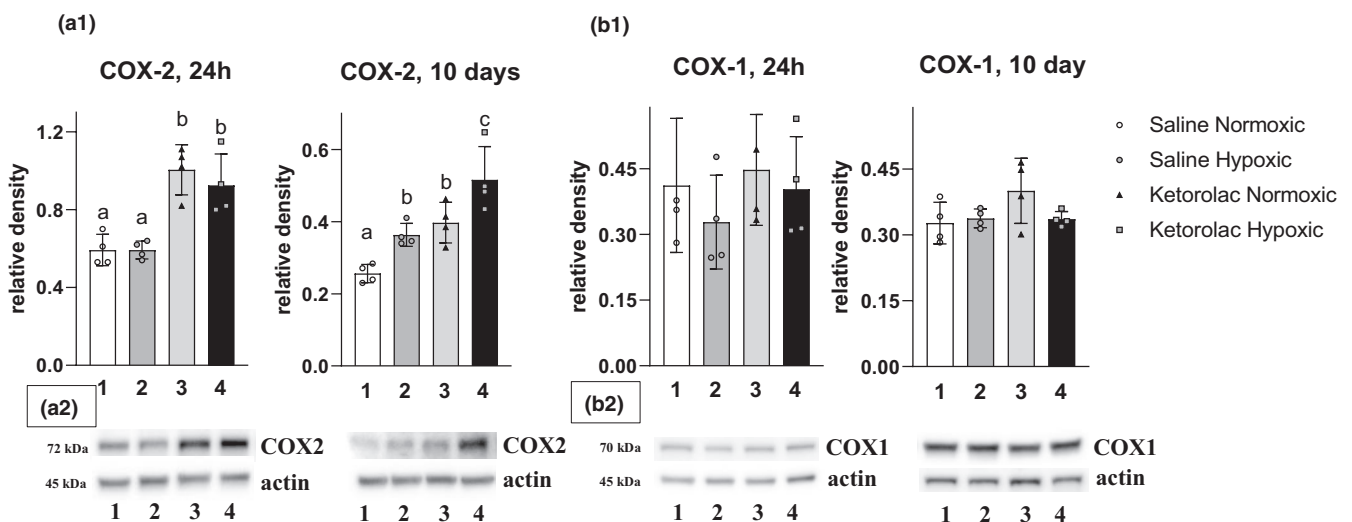


FIGURE 3 Brain COX alterations upon hypoxia and ketorolac treatment. Mice were treated with saline (1 and 2) or ketorolac (3 and 4) (s.c., osmotic pumps) under 24-hr or 10-day normoxia (1 and 3, $20\% \text{ O}_2$) or hypoxia (2 and 4, $10\% \text{ O}_2$). Brain COX-2 (panel a1) and COX-1 (panel b1) relative optical densities against actin were determined after western blot analysis. Panels a2 and b2 show representative blots for COX-2 and COX-1 analysis, respectively. Values are mean \pm standard deviation (n (number of animals) = 4) with individual values. Values that do not share the same letter are statistically different ($p < .05$, one-way ANOVA with Tukey's post hoc test)

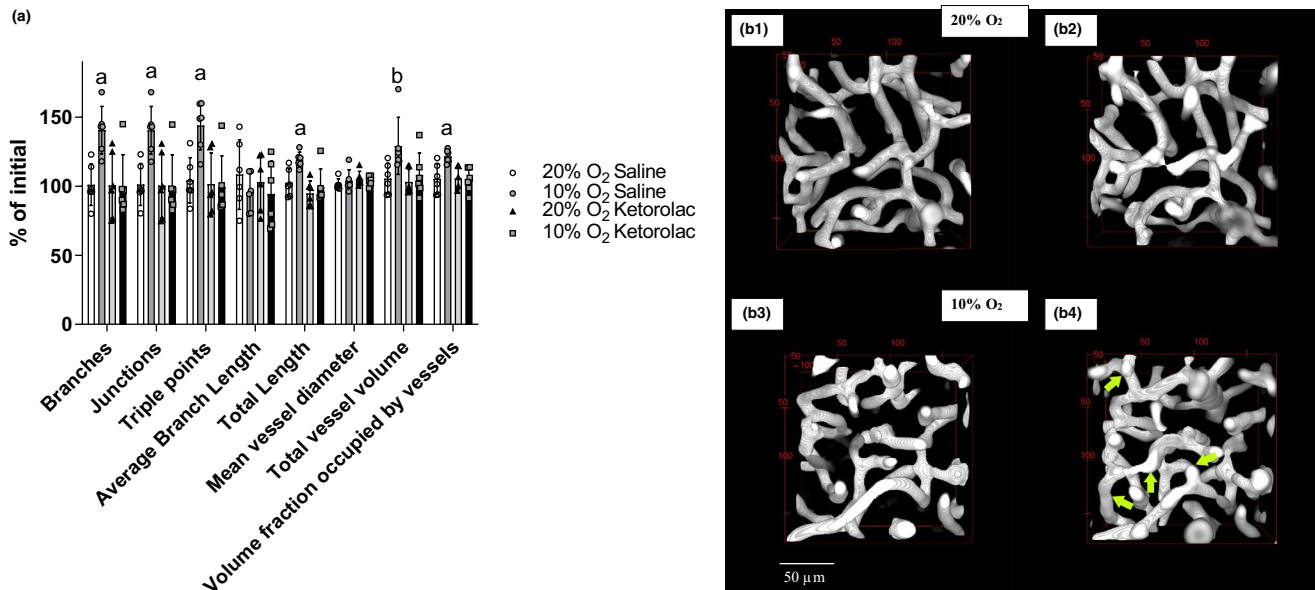


FIGURE 4 COX inhibition with ketorolac attenuates hypoxia-induced angiogenesis in the brain. Mouse transcranial vasculature over somatosensory cortex was imaged through thinned skull with multiphoton microscopy 2.5 days before exposure to isobaric normoxia (20% O₂) or hypoxia (10% O₂). Osmotic pumps containing saline (vehicle control) or ketorolac (infusion rate 0.62 mg kg⁻¹ h⁻¹) were implanted 0.5 days before hypoxia or normoxia treatment. At 10-day normoxia or hypoxia treatment, transcranial vascular was re-imaged from the same brain area. Conjugated TRITC-dextran was injected to visualize brain vasculature during first imaging, and conjugated FITC-dextran was injected during re-imaging to reduce background noise from previously injected dye. The 3D Z-stack images were analyzed using a TubeAnalyst macro (IRB Barcelona) available for Fiji (Image J) software. (a): Data are expressed as % change from initial values. Values are mean ± standard deviation (*n* (number of animals) = 6) with individual values. (a) - statistically different from all other conditions; (b) - statistically different from other conditions except for hypoxia ketorolac treatment (*p* < .05, one-way ANOVA with Tukey's post hoc test). (b): Representative image areas of transcranial vasculature before (b1 and b3) and after (b2 and b4) exposure to normoxia (b2) or hypoxia (b4). Dynamic changes are mark with yellow arrows

and volume fraction occupied by vessels (~1.2-fold, Figure 4 a and b). Consistent with previous reports (Benderro & LaManna, 2014; Cramer et al., 2019; Harb et al., 2013; Harik et al., 1996; Masamoto et al., 2013; Ward et al., 2007), these data indicate a significant induction of brain angiogenesis under mild chronic hypoxia.

COX inhibition with chronic ketorolac infusion (0.64 mg kg⁻¹ h⁻¹) completely attenuated hypoxia-induced angiogenesis, but did not affect brain vessels under normoxia (Figure 4, a and b), indicating a crucial role of COX in brain angioplasticity under hypoxia.

3.5 | Angiogenic factor alterations under hypoxia and ketorolac treatment

COX inhibition might affect angiogenesis through a number of different mechanisms. Because HIF-1α is considered to be a master regulator in tissue response to hypoxia including angiogenesis (Dvorak, 2005; Madrigal-Martinez et al., 2018; Sharp & Bernaudin, 2004), and was shown to be COX-dependent in some angiogenesis models (Jung et al., 2003; Kaidi et al., 2006; Liu et al., 2002; Zhong et al., 2004), we first determined HIF-1α alterations under hypoxia and ketorolac treatment. Consistent with previous studies (Benderro & LaManna, 2014; Ward et al., 2007), we detected a slight but significant increase in HIF-1α upon 24-hr and 10-day hypoxia (Figure 5a). However, HIF-1α was unaffected by ketorolac under

these conditions, indicating a HIF-1α-independent mechanism for the effect of COX on hypoxia-induced brain angiogenesis.

Another strong regulator for brain angiogenesis is VEGF/VEGFR2 signaling, which is significantly up-regulated under brain hypoxia (Benderro & LaManna, 2014; Esposito et al., 2018; Fan et al., 2018; Jun et al., 2020; Ndubuizu et al., 2010; Ward et al., 2007; Zhang et al., 2000) and was also reported to be COX-dependent in cancer cells (Fukuda et al., 2003; Jurek et al., 2004; Tsujii et al., 1998; Tuncer & Banerjee, 2015; Zhao et al., 2012). Consistent with previous studies, VEGF was dramatically increased by 2.1-fold under 24-hr hypoxia and remained elevated by 1.4-fold at 10-day hypoxia (Figure 5b). Ketorolac had no effect on VEGF under normoxia and 10-day hypoxia, but significantly potentiated VEGF induction under 24-hr hypoxia, probably as a compensatory effect of reduced angiogenic response.

The brain VEGFR2 response to hypoxia was delayed compared to the VEGF response, with a significant 2.3-fold increase in VEGFR2 at 10-day hypoxia only (Figure 5b). Ketorolac treatment had no effect under normoxia and 24-hr hypoxia; however, it significantly attenuated VEGFR2 levels at 10-day hypoxia by 40%. Importantly, VEGFR2 levels were still 2.2-fold higher upon 10-day ketorolac treatment under hypoxia compared to ketorolac normoxia (Figure 5b). Together with VEGF results, these data indicate that COX effect on VEGF/VEGFR2 signaling is not the primary mechanism for angiogenesis regulation under brain hypoxia.

We also measured bFGF/FGFR1 alterations under brain hypoxia and ketorolac treatment (Figure 5c). bFGF/FGFR1 strongly promotes

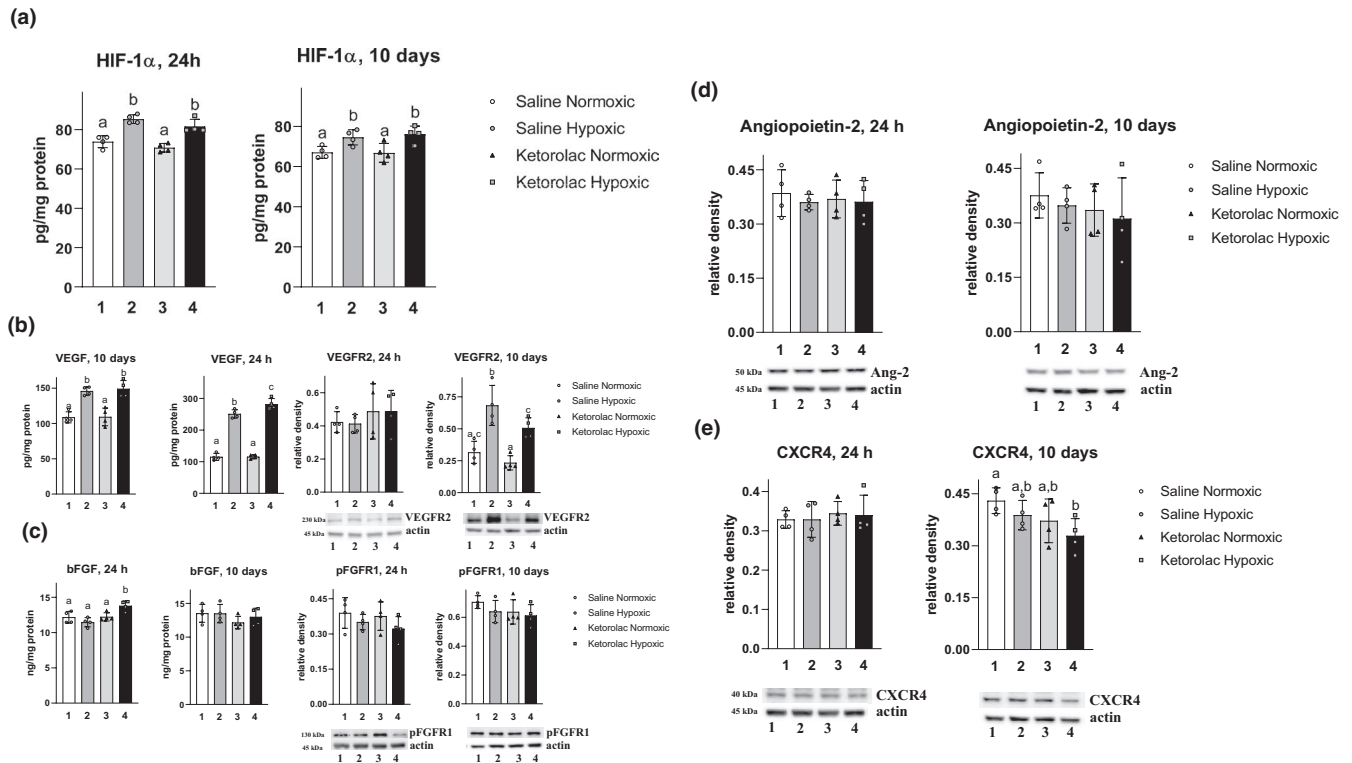


FIGURE 5 Alterations in brain angiogenic factor under hypoxia and COX inhibition with ketorolac. Mice were treated with saline (1 and 2) or ketorolac (3 and 4) using osmotic pumps (s.c.) under 24-hr or 10-day normoxia (1 and 3, 20% O₂) or hypoxia (2 and 4, 10% O₂). Values are mean \pm standard deviation (n (number of animals) = 4) with individual values. Values that do not share the same letter are statistically different ($p < .05$, one-way ANOVA with Tukey's post hoc test). (a) COX inhibition with ketorolac has no effect on HIF-1 α levels under brain hypoxia as determined using ELISA. (b) COX inhibition with ketorolac has a slight but significant effect on brain VEGF and VEGFR2 levels under hypoxia. Brain VEGF was determined using ELISA. VEGFR2 were determined after western blot analysis and relative optical densities against actin are presented. Panels below bar graphs show representative blots for VEGFR2. (c) COX inhibition with ketorolac has no effect on brain bFGF and FGFR1 levels under hypoxia. Brain bFGF was determined using ELISA. pFGFR1 was determined after western blot analysis and relative optical densities against actin are presented. Panels below bar graphs show representative blots for pFGFR1. (d) COX inhibition with ketorolac has no effect on brain angiopoietin-2 under hypoxia. Brain angiopoietin-2 (Ang-2) was determined after western blot analysis and expressed as relative optical densities against actin. Panels below bar graphs show representative blots for Ang-2. (e) COX inhibition with ketorolac slightly but significantly attenuates CXCR4 after 10-day hypoxia. Brain CXCR4 was determined after western blot analysis and expressed as relative optical densities against actin. Panels below bar graphs show representative blots for CXCR4

angiogenesis in different models such as endothelial cultures, tumor cells, chick embryo chorioallantoic membrane, and mouse cornea (Conconi et al., 2004; Katori et al., 1998; Leahy et al., 2000; Nakatsu et al., 2003; Presta et al., 1986; Thompson et al., 1988), and several studies indicated bFGF/FGFR1 regulation through COX activity (Finetti et al., 2008; Katori et al., 1998; Leahy et al., 2000). However, to the best of our knowledge, no previous studies addressed this signaling in brain tissue under hypoxia. bFGF and activated pFGFR1 were unchanged under hypoxia or ketorolac treatment, indicating a limited role for this mechanism for brain hypoxia-induced angiogenicity.

Another potent mechanism for angiogenesis induction in different systems including brain is angiopoietin (Jun et al., 2020; Nakatsu et al., 2003; Pichiule & LaManna, 2002; Simon et al., 2008; Ward et al., 2007). Angiopoietin-2 was reported to be COX dependent in brain germinal matrix but not in other brain structures (Kang et al., 2007). However, contrary to previous report (Benderro & LaManna, 2011), we did not find significant alterations in

angiopoietin-2 under hypoxia (Figure 5d). Angiopoietin-2 was also unchanged under ketorolac treatment (Figure 5d).

Finally, we measured CXCR4, which has been reported to be PGE₂ dependent (Salcedo et al., 2003). However, to the best of our knowledge, no previous studies addressed CXCR4 levels under brain hypoxia. Similar to bFGF/FGFR1 and angiopoietin-2, we did not find significant CXCR4 alterations under brain hypoxia or upon COX inhibition with ketorolac under hypoxia (Figure 5e). However, the combination of 10-day hypoxia with ketorolac treatment resulted in a slight (25%) but significant reduction in CXCR4 levels (Figure 5e). These data indicate that this is probably not the primary mechanism for COX-mediated brain angiogenicity.

3.6 | MAPK alterations upon ketorolac treatment

Because of the limited ketorolac effect on VEGF/bFGF/CXCR4/Angiopoietin-2 signaling mechanism, we tested if COX inhibition



altered MAPK members that are required to transduce the signals generated by growth factors, cytokines, and other stress factors to stimulate endothelial cell migrations and proliferation as critical steps of angiogenesis (Matsumoto et al., 1999; Mavria et al., 2006; Medhora et al., 2008; Rousseau et al., 1997). In turn, MAPK members are regulated by COX products (Cho & Choe, 2020; Riquelme et al., 2015), suggesting a possible alteration in MAPK upon COX inhibition.

Ketorolac had no significant effect on ERK1, p-ERK1, ERK2, p-ERK2, p38, p-p38, and SAPK/JNK under 24-hr hypoxia or normoxia (Figure S1). However, ketorolac significantly reduced activated p-ERK2, p38, and activated p-p38 by 25%–35% under 10-day hypoxia compared to saline-treated normoxic brains, and p-ERK2 and p-p38 compared to saline-treated hypoxic brains (Figure 6). ERK1, p-ERK1, ERK2, and SAPK/JNK were still unchanged at 10-day hypoxia (Figure S1). These data indicate that COX inhibition might attenuate brain angiogenesis through the effect on activated ERK2 and p38 levels.

4 | DISCUSSION

Previous studies reported increased COX-2 levels in the brain tissue under chronic hypoxia (Benderro & LaManna, 2014; LaManna et al., 2006), the conditions that promote brain angiogenesis (Benderro & LaManna, 2014; Cramer et al., 2019; Ward et al., 2007). Together with a hypothesized role for COX in cancer-induced angiogenesis, the role for COX in brain physiological angiogenesis was proposed (Benderro & LaManna, 2014; LaManna et al., 2006). However, to the best of our knowledge, no direct studies addressed the role for COX activity in brain angioplasticity. In the present study, we demonstrate, for the first time, that BBB COX inhibition completely inhibits brain angiogenesis under chronic hypoxia. In addition, we demonstrate that COX activity is required for survival under chronic hypoxia.

To induce angiogenic response in the brain, we used a well-documented model of chronic hypoxia. Both hypobaric (Benderro & LaManna, 2014; Cramer et al., 2019; Harik et al., 1996; Ndubuizu et al., 2010; Pichiule & LaManna, 2002; Ward et al., 2007) and isobaric (Harb et al., 2013; Masamoto et al., 2013) moderate hypoxia that corresponds to 9%–11% oxygen (α -50% reduction in breathing oxygen) induces brain angiogenesis as was documented using in vivo vasculature imaging (Harb et al., 2013; Masamoto et al., 2013), histochemical post-mortem staining against glucose transporters in brain vasculature (Benderro & LaManna, 2014; Harik et al., 1996; Ndubuizu et al., 2010; Pichiule & LaManna, 2002; Ward et al., 2007), or magnetic resonance angiography techniques (Cramer et al., 2019) to analyze the vascular density and morphology. Consistent with these studies, using in vivo multiphoton re-imaging technique after 10 days of moderate 50% isobaric hypoxia (10% oxygen by volume), we found a ~40% increase in the number of brain vesicular branches, junctions, triple points, and a ~20% increase in total vessel length, volume, and total volume fraction occupied by vessels without significant alterations in the average vessel diameter and branch length (Figure 4), indicating a significant induction of brain angiogenesis under these conditions.

To challenge the role for BBB COX activity in hypoxia-induced brain angiogenesis, we used the non-specific COX inhibitor ketorolac which was previously validated in our laboratory to not cross the BBB (Seeger et al., 2020). High doses of ketorolac (1.3 and 6.4 mg kg⁻¹ h⁻¹) completely inhibited PG synthesis in the mouse brain (Seeger et al., 2020) and significantly increased mortality rate in a dose-dependent manner (Figure 1) upon 10-day hypoxia but not normoxia with the deaths occurring between 9 and 10 days of hypoxia. These data indicate a critical role for COX activity in the systemic adaptation to global hypoxia. Because of high mortality rate, we did not quantify angiogenesis under high ketorolac dose. Lower 0.64 mg kg⁻¹ h⁻¹ drug dose was still toxic under hypoxia (Figure 1), but allowed for brain angiogenesis quantification. This dose inhibited ~82% of inducible PG production, and completely attenuated

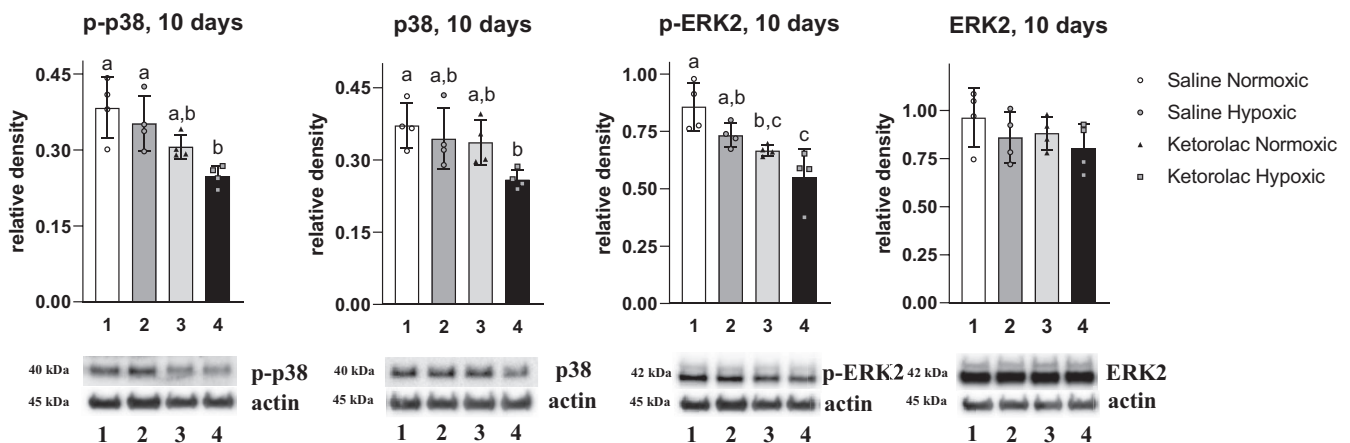


FIGURE 6 COX inhibition with ketorolac significantly attenuates brain p-p38, p38, and p-ERK2 MAPK after 10-day hypoxia. Mice were treated with saline (1 and 2) or ketorolac (3 and 4) (s.c., osmotic pumps) under 10-day normoxia (1 and 3, 20% O₂) or hypoxia (2 and 4, 10% O₂). Brain MAPK relative optical densities against actin were determined after western blot analysis. Values are mean \pm standard deviation (n (number of animals) = 4) with individual values. Values that do not share the same letter are statistically different ($p < .05$, one-way ANOVA with Tukey's post hoc test)

hypoxia-induced angiogenesis. Together, these data indicate a critical role of COX activity in adaptation to hypoxia, probably through multiple mechanisms including angiogenesis. Future studies are required to evaluate the clinical significance of these findings when treatment with COX inhibitors is used under low tissue oxygen supply like stroke, trauma, pulmonary disorders, and other similar conditions.

One of the importing findings in our study is a dose-dependent increase in mortality rate upon COX inhibition under hypoxia (Figure 1). Increased mortality under these conditions might be related to dysregulation of the cerebral blood flow (CBF). It is well documented that eicosanoids play a significant role in CBF autoregulation. However, this mechanism is rather convoluted and implicates COX as a source and regulator of a number of vasodilators and vasoconstrictors and their receptors. As part of arachidonic acid cascade, COX activity is required for producing CBF vasoactive PGs such as PGE₂, PGF_{2 α} , TXA₂, prostacyclins, and their receptors (Davidge, 2001; Li et al., 1997; Rebel et al., 2015). In addition, COX catabolizes P450 products that also regulate CBF, such as vasodilator epoxyeicosatrienoic acids, and vasoconstrictor 20-hydroxyeicosatetraenoic acid to produce vasoconstrictor endoperoxides or vasodilator prostanoids (Alkayed et al., 1996; Iliff et al., 2009, 2010; Imig, 2016; Toth et al., 2011; Zhang et al., 2008). Thus, it is difficult to predict the overall effect of COX inhibition on CBF that might be condition dependent. It has been demonstrated that COX inhibition attenuates myogenic middle cerebral artery constriction (Toth et al., 2011), thus contributing to CBF increase. Although COX inhibition decreases CBF under normoxia, it has no effect on CBF increase under hypoxia (Kellawan et al., 2019). Because of limited effect of COX inhibition on CBF under hypoxia (Kellawan et al., 2019), it is unlikely that COX role in CBF regulation is the only mechanism for increased mortality upon COX inhibition under hypoxia, and dysregulation of brain angiogenesis might also contribute to the decreased survival under these conditions.

Different mechanisms might account for the decreased angiogenesis upon COX inhibition including down-regulation of HIF. HIF is a well-documented master regulator for multiple angiogenic factors (Dvorak, 2005; Li et al., 2015; Madrigal-Martínez et al., 2018; Rabinovitch et al., 2017; Zhou et al., 2012), and alterations in HIF levels may have an effect on angiogenesis. In different cancer cell lines, non-selective COX inhibitors reduce HIF-1 α and -2 α levels in response to hypoxia (Jung et al., 2003) (Zhong et al., 2004) (Kaidi et al., 2006). It is possible that COX products, prostaglandins (PG), regulate HIF-1 α stabilization and nuclear localization as has been demonstrated for PGE₂ in a human prostate cancer cell line (Liu et al., 2002). However, the relation between HIF levels and COX activity is not completely established in all models and in some cases the effect of COX inhibition on angiogenesis might be independent from HIF pathway. For example, selective COX-2 inhibitor NS-398 does not significantly inhibit HIF-1 α accumulation in response to hypoxia in neither 'COX-2-positive' PC-3 cells, nor 'COX-2-negative' DU145 cells (Clendenon et al., 1985). In addition, different NSAIDs increase HIF-1 α expression in human gastric mucosa (Lamy & McNamara, 2003), and gene expression profiling and protein analysis in COX-2-containing and COX-2-silenced breast cancer cells

indicate minimal role for COX-2 in hypoxia-induced transcriptional response including HIF-1 α levels (Stasinopoulos et al., 2009). In the present study, we did not find an effect of non-selective COX inhibitor ketorolac on brain HIF-1 α levels under normoxia or hypoxia at early and late stages of drug treatment (Figure 5a). These data indicate that HIF-1 α pathway is independent from COX activity in the brain under hypoxia.

Another potential role for COX activity in brain angiogenesis is pro-angiogenic growth factor signaling regulation, including FGF and VEGF. Similar to other tissues, VEGF-A and VEGFR2 are strongly up-regulated under brain hypoxia and ischemia in rodents and have a critical role in adult brain angiogenesis (Benderro & LaManna, 2014; Esposito et al., 2018; Fan et al., 2018; Jun et al., 2020; Ndubuizu et al., 2010; Ward et al., 2007; Zhang et al., 2000). Consistent with previous reports, we demonstrated a strong VEGF-A and VEGFR2 up-regulation under early and late hypoxia in the brain (Figure 5b).

COX role in VEGF signaling was demonstrated in several angiogenesis studies, although the results are inconsistent across different models. In tumor-induced angiogenesis, exogenous PGE₂ strongly stimulates VEGF expression (Fukuda et al., 2003; Jurek et al., 2004; Tsujii et al., 1998; Tuncer & Banerjee, 2015). Similarly, *in vitro* studies on HUVEC cultures demonstrated that COX-2 inhibition with NS-398 attenuates VEGF levels, while exogenous PGE₂ reverses the inhibitory effects of NS-398 (Zhao et al., 2012). However, exogenous PGE₂ has no effect on VEGFR2 in microvascular endothelial cell cultures (Finetti et al., 2008), and COX-2 inhibition has no effect on VEGF levels in cortex or white matter in rabbit pups (Ballabh et al., 2007). Importantly, VEGF and bFGF signaling is additionally regulated through peroxisome proliferator-activated receptors (PPARs) (Bishop-Bailey, 2011; Piqueras et al., 2007; Wang et al., 2006) that is in turn up-regulated through another COX product PGD₂ and its non-enzymatic metabolite, Δ (12)-PGJ₂ (Fujimori, 2012), highlighting additional potential mechanism for angiogenesis regulation by COX activity. In the current study, we did not find a significant effect of COX inhibition on brain VEGF levels at 10-day hypoxia. A slight but significant increase in VEGF at early 24-hr hypoxia upon ketorolac treatment (Figure 5b) might be explained through compensatory over-expression under decreased angiogenic response upon COX inhibition. Although we found a slight but significant decrease in VEGFR2 levels at 10-day hypoxia, VEGFR2 levels were still 2.2-fold higher compared to normoxic ketorolac-treated brains (Figure 5b). These data indicate that VEGF/VEGFR signaling is unlikely involved in a complete angiogenesis attenuation upon COX inhibition.

bFGF is another well-documented angiogenic factor that promotes angiogenesis in different models such as endothelial cultures, tumor cells, chick embryo chorioallantoic membrane, and mouse cornea (Conconi et al., 2004; Katori et al., 1998; Leahy et al., 2000; Nakatsu et al., 2003; Presta et al., 1986; Thompson et al., 1988). Several studies indicate a role for COX in bFGF-mediated angiogenesis. In endothelial cell cultures, COX product PGE₂ selectively promotes angiogenesis through bFGF/FGFR1 signaling (Finetti et al., 2008) that involves FGFR1 activation through phosphorylation. Furthermore, COX inhibitors are anti-angiogenic in a bFGF-induced sponge implant model in rats (Katori et al., 1998). In a mouse



corneal micropocket angiogenesis assay induced with implanted pellet loaded with bFGF, oral NSAID administration (indomethacin, dexamethasone, or SC-236) inhibited bFGF-induced angiogenesis (Leahy et al., 2000), although it is difficult to differentiate between bFGF-induced angiogenesis and injury or inflammatory-associated angiogenic mechanisms in this model. However, to the best of our knowledge, no previous studies addressed bFGF levels in the adult brain under hypoxia. Surprisingly, we did find significant increase in brain bFGF under 24-hr or 10-day hypoxia (Figure 5c), indicating a higher contribution of VEGF signaling in hypoxia-induced angioplasticity in the brain. Similar to VEGF signaling, ketorolac had limited effect on FGF/FGFR levels. A slight induction in FGF at 10-day hypoxia upon ketorolac treatment might be explained through compensatory mechanism upon angiogenesis attenuation. Together, these data indicate that VEGF/VEGFR or bFGF/FGFR signaling is unlikely involved in a complete angiogenesis attenuation upon COX inhibition.

Alternatively, bFGF and VEGF up-regulate COX-2 expression in several cell lines and implanted sponge models (Goddard et al., 1992; Kage et al., 1999; Katori et al., 1998; Leahy et al., 2000; Sasaki et al., 1998), and indomethacin inhibits both bFGF-induced PGE₂ and angiogenesis in the egg chorioallantoic membrane (Spisni et al., 1992). These data indicate a positive feedback mechanism between COX and FGF/VEGF, but also might indicate that COX signaling is downstream from FGF/VEGF in angiogenic response and is an independent but essential contributor to angiogenic response.

Another mechanism for COX involvement in angiogenesis is angiopoietin/Tie-2 regulation. Angiopoietins are important angiogenic factor in different systems including brain (Jun et al., 2020; Nakatsu et al., 2003; Pichiule & LaManna, 2002; Simon et al., 2008; Ward et al., 2007) that facilitate VEGF-induced angiogenesis (Zhu et al., 2005). In the brain, angiopoietin-2 is considered to have a major role in angiopoietin/Tie-2 pathway (Benderro & LaManna, 2011; Benderro et al., 2012). Intriguingly, angiopoietin-2 is increased in both hyperoxic (Benderro et al., 2012) and hypoxic (Benderro & LaManna, 2011) mouse brain, indicating its dual role in brain angioplasticity. Angiopoietin-2 was reported to be COX dependent. In glioblastoma cells, selective COX-2 inhibitor celecoxib down-regulated angiopoietin-1 and angiopoietin-2 with reduction in VEGF and angiogenesis (Kang et al., 2007). Similarly, COX-2 inhibition reduced angiopoietin-2 levels in germinal matrix (Ballabh et al., 2007). However, in the same study, COX-2 inhibition had no effect on angiopoietin-2 in the cortex or white matter in rabbit pups (Ballabh et al., 2007). Because of possible relation between COX-2 and angiopoietin-2 levels, we tested the effect of COX inhibition on brain angiopoietin levels in hypoxic brains. We did not detect brain angiopoietin-2 alterations under hypoxia (Figure 5d), consistent with its decreased response to hypoxia in the adult brain (Benderro & LaManna, 2011). Ketorolac treatment had no effect on angiopoietin-2. These data indicate that COX might promote angiogenesis independently from angiopoietin-2 pathway in the adult hypoxic brain.

COX product, PGE₂, also up-regulates CXCR4 in human microvascular endothelial cells, and enhances cellular response to SDF-1, a unique ligand for CXCR4 (Salcedo et al., 2003). However, in this

model, NS-398 or piroxicam inhibited bFGF-induced angiogenesis by about 50% indicating COX-independent mechanisms for bFGF angiogenic effect. Moreover, high levels of CXCR4 are expressed in brain microvascular endothelial cells (Berger et al., 1999). However, to the best of our knowledge, no previous studies addressed CXCR-mediated angioplasticity in the normal or hypoxic brain. In the present study, we did not detect any significant induction in brain CXCR4 under hypoxia (Figure 5e), indicating a limited contribution of this receptor in hypoxia-induced brain angioplasticity. In addition, a limited but significant reduction in CXCR4 at 10-day hypoxia upon COX inhibition unlikely explains a complete attenuation in brain angiogenesis.

Together, these data indicate that BBB COX activity might contribute to brain hypoxia-mediated angiogenesis through independent VEGF/bFGF/CXCR4/Angiopoietin-2 mechanism. One of such mechanisms might be a direct mitogenic effect of COX products that controls endothelial cell proliferation and migration through MAPK pathway in addition to the discussed growth factors. It is well established that COX-2 product PGE₂ has a direct activating effect on proliferation in tumors (Pozzi et al., 2004; Sheng et al., 2001; Wang et al., 2004) and different normal cells including endothelial cells (Jumblatt, 1997; Jumblatt et al., 1988; Nordlund et al., 1986). PGE₂ might activate proliferation and migration through MAPK pathway because in cell cultures it activates p-p38 (Cho & Choe, 2020), p-ERK1, and p-ERK2 (Krysan et al., 2005; Riquelme et al., 2015). In turn, MAPK might stimulate PGE₂ production (Lo, 2003), indicating a positive feedback mechanism. Importantly, MAPK including ERK, SAPK/JNK, and p38 activation is required for angiogenic response *in vitro* (Matsumoto et al., 1999; Mavria et al., 2006; Medhora et al., 2008; Rousseau et al., 1997). These studies suggest a MAPK-mediated role for COX in angiogenesis. However, to the best of our knowledge, no studies addressed COX inhibition effect on brain MAPK *in vivo*. Our results demonstrate a significant decrease in p-ERK2, p38, and p-p38 upon 10-day hypoxia (Figure 6). Thus, it is possible that increased COX activity is an essential trigger for MAPK-mediated mitosis that is further controlled by specific growth factors. Further studies are required to elucidate if mitosis initiation is the primary mechanism for COX role in hypoxia-induced brain angioplasticity.

ACKNOWLEDGMENTS

This study was partially supported by NIH/NINDS grant 5R21NS109856 (M.Y.G.). LC-MS studies were conducted in the UND MS Core facility established with the NIH Grant 5P30GM103329-05 support (M.Y.G.) and supported by DaCCoTA CTR NIH grant U54GM128729 and UNDSMHS funds. Imaging studies were conducted in the UND Imaging Core facility supported by NIH grant P20GM113123, DaCCoTA CTR NIH grant U54GM128729, and UNDSMHS funds.

All experiments were conducted in compliance with the ARRIVE guidelines.

CONFLICT OF INTERESTS

The author(s) declare no potential conflict of interest with respect to the research, authorship, and/or publication of this article.

AUTHORS' CONTRIBUTIONS

DS performed the experiments, analyzed the results, participated in designing the study, writing the manuscript, and interpreting the results; SG developed MS approach, analyzed and interpreted MS data; BG assisted with imaging setup; MG designed and supervised the study, wrote the manuscript, analyzed and interpreted the results; all the authors critically revised and approved the final manuscript.

OPEN RESEARCH BADGES



This article has earned an Open Materials badge for making publicly available the components of the research methodology needed to reproduce the reported procedure and analysis. All materials are available at: <https://cos.io/our-services/open-science-badges/>.

ORCID

Drew R. Seeger  <https://orcid.org/0000-0002-9382-2753>

Mikhail Y. Golovko  <https://orcid.org/0000-0003-1749-3158>

REFERENCES

- Alexanian, A., & Sorokin, A. (2017). Cyclooxygenase 2: Protein-protein interactions and posttranslational modifications. *Physiological Genomics*, 49, 667–681. <https://doi.org/10.1152/physiolgenomics.00086.2017>
- Alkayed, N. J., Birks, E. K., Hudetz, A. G., Roman, R. J., Henderson, L., & Harder, D. R. (1996). Inhibition of brain P-450 arachidonic acid epoxidase decreases baseline cerebral blood flow. *American Journal of Physiology-Heart and Circulatory Physiology*, 271, H1541–H1546. <https://doi.org/10.1152/ajpheart.1996.271.4.H1541>
- Amy, M. R., & Katerina, D.-Z. (1996). Glomeruloid vascular structures in glioblastoma multiforme: An immunohistochemical and ultrastructural study. *Journal of Neurosurgery*, 85, 1078–1084. <https://doi.org/10.3171/jns.1996.85.6.1078>
- Ballabh, P., Xu, H., Hu, F., Braun, A., Smith, K., Rivera, A., Lou, N., Ungvari, Z., Goldman, S. A., Csiszar, A., & Nedergaard, M. (2007). Angiogenic inhibition reduces germinal matrix hemorrhage. *Nature Medicine*, 13, 477–485.
- Benderro, G. F., & LaManna, J. C. (2011). Hypoxia-induced angiogenesis is delayed in aging mouse brain. *Brain Research*, 1389, 50–60. <https://doi.org/10.1016/j.brainres.2011.03.016>
- Benderro, G. F., & LaManna, J. C. (2014). HIF-1 α /COX-2 expression and mouse brain capillary remodeling during prolonged moderate hypoxia and subsequent re-oxygenation. *Brain Research*, 1569, 41–47. <https://doi.org/10.1016/j.brainres.2014.04.035>
- Benderro, G. F., Sun, X., Kuang, Y., & LaManna, J. C. (2012). Decreased VEGF expression and microvascular density, but increased HIF-1 and 2 α accumulation and EPO expression in chronic moderate hyperoxia in the mouse brain. *Brain Research*, 1471, 46–55. <https://doi.org/10.1016/j.brainres.2012.06.055>
- Berger, O., Gan, X., Gujuluva, C., Burns, A. R., Sulur, G., Stins, M., Way, D., Witte, M., Weinand, M., Said, J., Kim, K. S., Taub, D., Graves, M. C., & Fiala, M. (1999). CXC and CC chemokine receptors on coronary and brain endothelia. *Molecular medicine (Cambridge, Mass.)*, 5, 795–805.
- Bishop-Bailey, D. (2011). PPARs and angiogenesis. *Biochemical Society Transactions*, 39, 1601–1605.
- Brose, S., Baker, A., & Golovko, M. (2013a). A fast one-step extraction and UPLC-MS/MS analysis for E2/D2 series prostaglandins and isoprostanes. *Lipids*, 48, 411–419. <https://doi.org/10.1007/s11745-013-3767-5>
- Brose, S. A., Baker, A. G., & Golovko, M. Y. (2013b). A fast one-step extraction and UPLC-MS/MS analysis for E2/D 2 series prostaglandins and isoprostanes. *Lipids*, 48, 411–419. <https://doi.org/10.1007/s11745-013-3767-5>
- Brose, S. A., & Golovko, M. Y. (2013). Eicosanoid post-mortem induction in kidney tissue is prevented by microwave irradiation. *Prostaglandins Leukotrienes and Essential Fatty Acids*, 89, 313–318. <https://doi.org/10.1016/j.plefa.2013.09.005>
- Brose, S. A., Golovko, S. A., & Golovko, M. Y. (2016). Brain 2-Arachidonoylglycerol levels are dramatically and rapidly increased under acute ischemia-injury which is prevented by microwave irradiation. *Lipids*, 51, 487–495. <https://doi.org/10.1007/s11745-016-4144-y>
- Brose, S. A., Thuen, B. T., & Golovko, M. Y. (2011). LC/MS/MS method for analysis of E2 series prostaglandins and isoprostanes. *Journal of Lipid Research*, 52, 850–859.
- Chen, J., Chen, J., Fu, H., Li, Y., Wang, L., Luo, S., & Lu, H. (2019). Hypoxia exacerbates nonalcoholic fatty liver disease via the HIF-2 α /PPAR α pathway. *American Journal of Physiology-Endocrinology and Metabolism*, 317, E710–E722. <https://doi.org/10.1152/ajpen.00052.2019>
- Cho, W., & Choe, J. (2020). Prostaglandin E2 stimulates COX-2 expression via mitogen-activated protein kinase p38 but not ERK in human follicular dendritic cell-like cells. *BMC Immunology*, 21, 20. <https://doi.org/10.1186/s12865-020-00347-y>
- Clendenon, N. R., Palayoor, S. T., Gordon, W. A., Zappia, V., Kennedy, E. P., Nilsson, B. I., & Galletti, P. (1985). Influence of CDPcholine on ATPase activity in acute experimental spinal cord trauma. *Novel Biochemical, Pharmacological and Clinical Aspects of Cytidinediphosphocholine* (pp. 275–284). Elsevier.
- Conconi, M. T., Nico, B., Guidolin, D., Baiguera, S., Spinazzi, R., Rebuffat, P., Malendowicz, L. K., Vacca, A., Carraro, G., Parnigotto, P. P., Nussdorfer, G. G., & Ribatti, D. (2004). Ghrelin inhibits FGF-2-mediated angiogenesis in vitro and in vivo. *Peptides*, 25, 2179–2185. <https://doi.org/10.1016/j.peptides.2004.08.011>
- Cramer, N. P., Korotcov, A., Bosomtvi, A., Xu, X., Holman, D. R., Whiting, K., Jones, S., Hoy, A., Dardzinski, B. J., & Galdzicki, Z. (2019). Neuronal and vascular deficits following chronic adaptation to high altitude. *Experimental Neurology*, 311, 293–304.
- Davidge, S. T. (2001). Prostaglandin H synthase and vascular function. *Circulation Research*, 89, 650–660.
- Ding, Y. H., Li, J., Zhou, Y., Rafols, J. A., Clark, J. C., & Ding, Y. (2006). Cerebral angiogenesis and expression of angiogenic factors in aging rats after exercise. *Current Neurovascular Research*, 3, 15–23.
- Dvorak, H. F. (2005). Angiogenesis: Update 2005. *Journal of Thrombosis and Haemostasis*, 3, 1835–1842. <https://doi.org/10.1111/j.1538-7836.2005.01361.x>
- Esposito, E., Hayakawa, K., Ahn, B. J., Chan, S. J., Xing, C., Liang, A. C., Kim, K.-W., Arai, K., & Lo, E. H. (2018). Effects of ischemic post-conditioning on neuronal VEGF regulation and microglial polarization in a rat model of focal cerebral ischemia. *Journal of Neurochemistry*, 146, 160–172. <https://doi.org/10.1111/jnc.14337>
- Fan, Y., Ding, S., Sun, Y., Zhao, B., Pan, Y., & Wan, J. (2018). MiR-377 regulates inflammation and angiogenesis in rats after cerebral ischemic injury. *Journal of Cellular Biochemistry*, 119, 327–337.
- Farias, S. E., Basselin, M., Chang, L., Heidenreich, K. A., Rapoport, S. I., & Murphy, R. C. (2008). Formation of eicosanoids, E2/D2 isoprostanes, and docosanoids following decapitation-induced ischemia, measured in high-energy-microwaved rat brain. *Journal of Lipid Research*, 49, 1990–2000.
- Ferrario, A., von Tiehl, K., Wong, S., Luna, M., & Gomer, C. J. (2002). Cyclooxygenase-2 inhibitor treatment enhances photodynamic therapy-mediated tumor response. *Cancer Research*, 62, 3956–3961.
- Finetti, F., Solito, R., Morbidelli, L., Giachetti, A., Ziche, M., & Donnini, S. (2008). Prostaglandin E2 regulates angiogenesis via activation of



- fibroblast growth factor receptor-1. *Journal of Biological Chemistry*, 283, 2139–2146.
- Fujimori, K. (2012). Prostaglandins as PPAR γ modulators in adipogenesis. *PPAR Research*, 2012, 527607.
- Fukuda, R., Kelly, B., & Semenza, G. L. (2003). Vascular endothelial growth factor gene expression in colon cancer cells exposed to prostaglandin e₂ is mediated by hypoxia-inducible factor 1. *Cancer Research*, 63, 2330.
- Goddard, D. H., Grossman, S. L., Newton, R., Clark, M. A., & Bomalaski, J. S. (1992). Regulation of synovial cell growth: Basic fibroblast growth factor synergizes with interleukin 1 β stimulating phospholipase A2 enzyme activity, phospholipase A2 activating protein production and release of prostaglandin E2 by rheumatoid arthritis synovial cells in culture. *Cytokine*, 4, 377–384. [https://doi.org/10.1016/1043-4666\(92\)90081-2](https://doi.org/10.1016/1043-4666(92)90081-2)
- Golovko, M. Y., & Murphy, E. J. (2008a). Brain prostaglandin formation is increased by α -synuclein gene-ablation during global ischemia. *Neuroscience Letters*, 432, 243–247.
- Golovko, M. Y., & Murphy, E. J. (2008b). An improved LC-MS/MS procedure for brain prostanoid analysis using brain fixation with head-focused microwave irradiation and liquid-liquid extraction. *Journal of Lipid Research*, 49, 893–902. <https://doi.org/10.1194/jlr.D700030-JLR200>
- Harb, R., Whiteus, C., Freitas, C., & Grutzendler, J. (2013). In vivo imaging of cerebral microvascular plasticity from birth to death. *Journal of Cerebral Blood Flow and Metabolism: Official Journal of the International Society of Cerebral Blood Flow and Metabolism*, 33, 146–156.
- Harik, N., Harik, S. I., Kuo, N.-T., Sakai, K., Przybylski, R. J., & LaManna, J. C. (1996). Time-course and reversibility of the hypoxia-induced alterations in cerebral vascularity and cerebral capillary glucose transporter density. *Brain Research*, 737, 335–338. [https://doi.org/10.1016/0006-8993\(96\)00965-1](https://doi.org/10.1016/0006-8993(96)00965-1)
- Iliff, J. J., Jia, J., Nelson, J., Goyagi, T., Klaus, J., & Alkayed, N. J. (2010). Epoxyeicosanoid signaling in CNS function and disease. *Prostaglandins & Other Lipid Mediators*, 91, 68–84. <https://doi.org/10.1016/j.prostaglandins.2009.06.004>
- Iliff, J. J., Wang, R., Zeldin, D. C., & Alkayed, N. J. (2009). Epoxyeicosanoids as mediators of neurogenic vasodilation in cerebral vessels. *American Journal of Physiology-Heart and Circulatory Physiology*, 296, H1352–H1363. <https://doi.org/10.1152/ajpheart.00950.2008>
- Imig, J. D. (2016). Epoxyeicosatrienoic acids and 20-hydroxyeicosatetraenoic acid on endothelial and vascular function. *Advances in pharmacology (San Diego, Calif.)*, 77, 105–141.
- Jalota, A., Kumar, M., Das, B. C., Yadav, A. K., Chosdol, K., & Sinha, S. (2018). A drug combination targeting hypoxia induced chemoresistance and stemness in glioma cells. *Oncotarget*, 9, 18351–18366. <https://doi.org/10.18632/oncotarget.24839>
- Jumblatt, M. M. (1997). PGE2 synthesis and response pathways in cultured corneal endothelial cells: The effects of in vitro aging. *Current Eye Research*, 16, 428–435. <https://doi.org/10.1076/ceyr.16.5.428.7048>
- Jumblatt, M. M., Matkin, E. D., & Neufeld, A. H. (1988). Pharmacological regulation of morphology and mitosis in cultured rabbit corneal endothelium. *Investigative Ophthalmology & Visual Science*, 29, 586–593.
- Jun, Y. H., Ju, G. S., Chung, Y. Y., Shin, H.-K., Kim, D.-J., Choi, M. S., Kim, S. T., & Son, K. M. (2020). Differential expression of vascular endothelial growth factor in the cortex and hippocampus upon cerebral hypoperfusion. *Vivo*, 34, 191–197. <https://doi.org/10.21873/invivo.11761>
- Jung, Y.-J., Isaacs, J. S., Lee, S., Trepel, J., & Neckers, L. (2003). IL-1 β mediated up-regulation of HIF-1 α via an NF κ B/COX-2 pathway identifies HIF-1 as a critical link between inflammation and oncogenesis. *The FASEB Journal*, 17, 1–22. <https://doi.org/10.1096/fj.03-0329fje>
- Jurek, D., Udilova, N., Jozkowicz, A., Nohl, H., Marian, B., & Schulte-Hermann, R. (2004). Dietary lipid hydroperoxides induce expression of vascular endothelial growth factor (VEGF) in human colorectal tumor cells. *The FASEB Journal*, 19, 97–99. <https://doi.org/10.1096/fj.04-2111fje>
- Kage, K., Fujita, N., Oh-hara, T., Ogata, E., Fujita, T., & Tsuruo, T. (1999). Basic fibroblast growth factor induces cyclooxygenase-2 expression in endothelial cells derived from bone. *Biochemical and Biophysical Research Communications*, 254, 259–263.
- Kaidi, A., Qualtrough, D., Williams, A. C., & Paraskeva, C. (2006). Direct transcriptional up-regulation of cyclooxygenase-2 by hypoxia-inducible factor (HIF)-1 promotes colorectal tumor cell survival and enhances HIF-1 transcriptional activity during hypoxia. *Cancer Research*, 66, 6683–6691. <https://doi.org/10.1158/0008-5472.CAN-06-0425>
- Kang, K. B., Wang, T. T., Woon, C. T., Cheah, E. S., Moore, X. L., Zhu, C., & Wong, M. C. (2007). Enhancement of glioblastoma radioresponse by a selective COX-2 inhibitor celecoxib: Inhibition of tumor angiogenesis with extensive tumor necrosis. *International Journal of Radiation Oncology Biology Physics*, 67, 888–896.
- Katoh, H., Hosono, K., Ito, Y., Suzuki, T., Ogawa, Y., Kubo, H., Kamata, H., Mishima, T., Tamaki, H., Sakagami, H., Sugimoto, Y., Narumiya, S., Watanabe, M., & Majima, M. (2010). COX-2 and prostaglandin EP3/EP4 signaling regulate the tumor stromal proangiogenic microenvironment via CXCL12-CXCR4 chemokine systems. *The American Journal of Pathology*, 176, 1469–1483. <https://doi.org/10.2353/ajpath.2010.090607>
- Katori, M., Majima, M., & Harada, Y. (1998). Possible background mechanisms of the effectiveness of cyclooxygenase-2 inhibitors in the treatment of rheumatoid arthritis. *Inflammation Research*, 47, 107–111.
- Kellawan, J. M., Peltonen, G. L., Harrell, J. W., Roldan-Alzate, A., Wieben, O., & Schrage, W. G. (2019). Differential contribution of cyclooxygenase to basal cerebral blood flow and hypoxic cerebral vasodilation. *American Journal of Physiology-Regulatory, Integrative and Comparative Physiology*, 318, R468–R479.
- Kleihues, P., Louis, D. N., Scheithauer, B. W., Rorke, L. B., Reifenberger, G., Burger, P. C., & Cavenee, W. K. (2002). The WHO classification of tumors of the nervous system. *Journal of Neuropathology and Experimental Neurology*, 61, 215–225.
- Krysan, K., Reckamp, K. L., Dalwadi, H., Sharma, S., Rozengurt, E., Kohadwala, M., & Dubinett, S. M. (2005). Prostaglandin E₂ activates mitogen-activated protein Kinase/Erk pathway signaling and cell proliferation in non-small cell lung cancer cells in an epidermal growth factor receptor-independent manner. *Cancer Research*, 65, 6275.
- LaManna, J. C. (2018). Cerebral angioplasticity: The anatomical contribution to ensuring appropriate oxygen transport to brain. *Advances in Experimental Medicine and Biology*, 1072, 3–6.
- LaManna, J. C., Sun, X., Ivy, A. D., & Ward, N. L. (2006). Is cyclooxygenase-2 (COX-2) a major component of the mechanism responsible for microvascular remodeling in the brain? *Advances in Experimental Medicine and Biology*, 578, 297–303.
- Lamy, V., & McNamara, D. (2003). Gastroenterology and hepatology services in Europe. *Alimentary Pharmacology & Therapeutics*, 18, 90–92.
- Leahy, K. M., Koki, A. T., & Masferrer, J. L. (2000). Role of cyclooxygenases in angiogenesis. *Current Medicinal Chemistry*, 7, 1163–1170.
- Lee, E. J., Choi, E. M., Kim, S. R., Park, J. H., Kim, H., Ha, K. S., Kim, Y. M., Kim, S. S., Choe, M., Kim, J., & Han, J. A. (2007). Cyclooxygenase-2 promotes cell proliferation, migration and invasion in U2OS human osteosarcoma cells. *Experimental & Molecular Medicine*, 39, 469–476.
- Li, D.-Y., Hardy, P., Abran, D., Martinez-Bermudez, A. K., Guerguerian, A. M., Bhattacharya, M., Almazan, G., Menezes, R., Peri, K. G., Varma, D. R., & Chemtob, S. (1997). Key role for cyclooxygenase-2 in PGE2 and PGF2 α receptor regulation and cerebral blood flow of the newborn. *American Journal of Physiology-Regulatory, Integrative and Comparative Physiology*, 273, R1283–R1290.

- Li, G., Yang, T., & Yan, J. (2002). Cyclooxygenase-2 increased the angiogenic and metastatic potential of tumor cells. *Biochemical and Biophysical Research Communications*, 299, 886–890.
- Li, H., Satriano, J., Thomas, J. L., Miyamoto, S., Sharma, K., Pastor-Soler, N. M., Hallows, K. R., & Singh, P. (2015). Interactions between HIF-1 α and AMPK in the regulation of cellular hypoxia adaptation in chronic kidney disease. *American Journal of Physiology - Renal Physiology*, 309, F414–F428. <https://doi.org/10.1152/ajprenal.00463.2014>
- Licht, T., Goshen, I., Avital, A., Kreisel, T., Zubedat, S., Eavri, R., Segal, M., Yirmiya, R., & Keshet, E. (2011). Reversible modulations of neuronal plasticity by VEGF. *Proceedings of the National Academy of Sciences of the United States of America*, 108, 5081–5086.
- Liu, X. H., Kirschenbaum, A., Lu, M., Yao, S., Dosoretz, A., Holland, J. F., & Levine, A. C. (2002). Prostaglandin E2 induces hypoxia-inducible factor-1 α stabilization and nuclear localization in a human prostate cancer cell line. *Journal of Biological Chemistry*, 277, 50081–50086.
- Lo, C.-J. (2003). Mapk regulation of prostaglandin E2 production by lipopolysaccharide-stimulated macrophages is not dependent on nuclear factor κ B22This study was support in part by a grant (NSC 91-2314-B-371-003) from National Science Counsel. *The Journal of Surgical Research*, 113, 189–194.
- Madrígal-Martínez, A., Fernández-Martínez, A. B., & Lucio Cazaña, F. J. (2018). Intracrine prostaglandin E2 pro-tumoral actions in prostate epithelial cells originate from non-canonical pathways. *Journal of Cellular Physiology*, 233, 3590–3602.
- Masamoto, K., Takuwa, H., Tomita, Y., Toriumi, H., Uekawa, M., Taniguchi, J., Kawaguchi, H., Itoh, Y., Suzuki, N., Ito, H., & Kanno, I. (2013). Hypoxia-induced cerebral angiogenesis in mouse cortex with two-photon microscopy. In S. Van Huffel, G. Naulaers, A. Caicedo, D. F. Bruley, & D. K. Harrison (Eds.), *Oxygen Transport to Tissue XXXV* (pp. 15–20). Springer.
- Matsumoto, T., Yokote, K., Tamura, K., Takemoto, M., Ueno, H., Saito, Y., & Mori, S. (1999). Platelet-derived growth factor activates p38 mitogen-activated protein kinase through a Ras-dependent pathway that is important for actin reorganization and cell migration. *Journal of Biological Chemistry*, 274, 13954–13960.
- Mavria, G., Vercoulen, Y., Yeo, M., Paterson, H., Karasarides, M., Marais, R., Bird, D., & Marshall, C. J. (2006). ERK-MAPK signaling opposes Rho-kinase to promote endothelial cell survival and sprouting during angiogenesis. *Cancer Cell*, 9, 33–44. <https://doi.org/10.1016/j.ccr.2005.12.021>
- Medhora, M., Dhanasekaran, A., Pratt, P. F. Jr, Cook, C. R., Dunn, L. K., Gruenloh, S. K., & Jacobs, E. R. (2008). Role of JNK in network formation of human lung microvascular endothelial cells. *American Journal of Physiology. Lung Cellular and Molecular Physiology*, 294, L676–685. <https://doi.org/10.1152/ajplung.00496.2007>
- Morland, C., Andersson, K. A., Haugen, Ø. P., Hadzic, A., Kleppa, L., Gille, A., Rinholm, J. E., Palibrk, V., Diget, E. H., Kennedy, L. H., Stølen, T., Hennestad, E., Moldestad, O., Cai, Y., Puchades, M., Offermanns, S., Vervaeke, K., Bjørås, M., Wisløff, U., ... Bergersen, L. H. (2017). Exercise induces cerebral VEGF and angiogenesis via the lactate receptor HCAR1. *Nature Communications*, 8, 15557. <https://doi.org/10.1038/ncomms15557>
- Nakatsu, M. N., Sainson, R. C. A., Aoto, J. N., Taylor, K. L., Aitkenhead, M., Pérez-del-Pulgar, S., Carpenter, P. M., & Hughes, C. C. W. (2003). Angiogenic sprouting and capillary lumen formation modeled by human umbilical vein endothelial cells (HUVEC) in fibrin gels: The role of fibroblasts and Angiopoietin-1. *Microvascular Research*, 66, 102–112. [https://doi.org/10.1016/S0026-2862\(03\)00045-1](https://doi.org/10.1016/S0026-2862(03)00045-1)
- Ndubuizu, O. I., Tshipis, C. P., Li, A., & LaManna, J. C. (2010). Hypoxia-inducible factor-1 (HIF-1)-independent microvascular angiogenesis in the aged rat brain. *Brain Research*, 1366, 101–109. <https://doi.org/10.1016/j.brainres.2010.09.064>
- Nordlund, J. J., Collins, C. E., & Rheins, L. A. (1986). Prostaglandin E2 and D2 but Not MSH stimulate the proliferation of pigment cells in the pinnal epidermis of the DBA/2 mouse. *The Journal of Investigative Dermatology*, 86, 433–437. <https://doi.org/10.1111/1523-1747.ep12285717>
- Percie du Sert, N., Hurst, V., Ahluwalia, A., Alam, S., Avey, M. T., Baker, M., Browne, W. J., Clark, A., Cuthill, I. C., Dirnagl, U., Emerson, M., Garner, P., Holgate, S. T., Howells, D. W., Karp, N. A., Lázic, S. E., Lidster, K., MacCallum, C. J., Macleod, M., ... Würbel, H. (2020). The ARRIVE guidelines 2.0: Updated guidelines for reporting animal research. *PLOS Biology*, 18, e3000410.
- Pichiule, P., & LaManna, J. C. (2002). Angiotensin-2 and rat brain capillary remodeling during adaptation and deadaptation to prolonged mild hypoxia. *Journal of Applied Physiology*, 93, 1131–1139.
- Piqueras, L., Reynolds Andrew, R., Hodivala-Dilke Kairbaan, M., Alfranca, A., Redondo Juan, M., Hatae, T., Tanabe, T., Warner Timothy, D., & Bishop-Bailey, D. (2007). Activation of PPAR β / δ induces endothelial cell proliferation and angiogenesis. *Arteriosclerosis, Thrombosis, and Vascular Biology*, 27, 63–69.
- Pozzi, A., Yan, X., Macias-Perez, I., Wei, S., Hata, A. N., Breyer, R. M., Morrow, J. D., & Capdevila, J. H. (2004). Colon carcinoma cell growth is associated with prostaglandin E2/EP4 receptor-evoked ERK activation. *Journal of Biological Chemistry*, 279, 29797–29804.
- Presta, M., Moscatelli, D., Joseph-Silverstein, J., & Rifkin, D. B. (1986). Purification from a human hepatoma cell line of a basic fibroblast growth factor-like molecule that stimulates capillary endothelial cell plasminogen activator production, DNA synthesis, and migration. *Molecular and Cellular Biology*, 6, 4060. <https://doi.org/10.1128/MCB.6.11.4060>
- Rabinovitch, R. C., Samborska, B., Faubert, B., Ma, E. H., Gravel, S.-P., Andrzejewski, S., Raissi, T. C., Pause, A., St-Pierre, J., & Jones, R. G. (2017). AMPK maintains cellular metabolic homeostasis through regulation of mitochondrial reactive oxygen species. *Cell Reports*, 21, 1–9. <https://doi.org/10.1016/j.celrep.2017.09.026>
- Rebel, A. A., Urquhart, S. A., Puig, K. L., Ghatak, A., Brose, S. A., Golovko, M. Y., & Combs, C. K. (2015). Brain changes associated with thromboxane receptor antagonist SQ 29,548 treatment in a mouse model. *Journal of Neuroscience Research*, 93, 1279–1292.
- Riquelme, M. A., Burra, S., Kar, R., Lampe, P. D., & Jiang, J. X. (2015). Mitogen-activated protein kinase (MAPK) activated by prostaglandin E2 phosphorylates connexin 43 and closes osteocytic hemichannels in response to continuous flow shear stress. *Journal of Biological Chemistry*, 290, 28321–28328.
- Rousseau, S., Houle, F., Landry, J., & Huot, J. (1997). p38 MAP kinase activation by vascular endothelial growth factor mediates actin reorganization and cell migration in human endothelial cells. *Oncogene*, 15, 2169–2177. <https://doi.org/10.1038/sj.onc.1201380>
- Salcedo, R., Zhang, X., Young, H. A., Michael, N., Wasserman, K., Ma, W.-H., Martins-Green, M., Murphy, W. J., & Oppenheim, J. J. (2003). Angiogenic effects of prostaglandin E2 are mediated by up-regulation of CXCR4 on human microvascular endothelial cells. *Blood*, 102, 1966–1977. <https://doi.org/10.1182/blood-2002-11-3400>
- Sasaki, E., Pai, R., Halter, F., Komurasaki, T., Arakawa, T., Kobayashi, K., Kuroki, T., & Tarnawski, A. S. (1998). Induction of cyclooxygenase-2 in a rat gastric epithelial cell line by epiregulin and basic fibroblast growth factor. *Journal of Clinical Gastroenterology*, 27, S21–S27. <https://doi.org/10.1097/00004836-199800001-00005>
- Schindelin, J., Arganda-Carreras, I., Frise, E., Kaynig, V., Longair, M., Pietzsch, T., Preibisch, S., Rueden, C., Saalfeld, S., Schmid, B., Tinevez, J.-Y., White, D. J., Hartenstein, V., Eliceiri, K., Tomancak, P., & Cardona, A. (2012). Fiji: An open-source platform for biological-image analysis. *Nature Methods*, 9, 676–682. <https://doi.org/10.1038/nmeth.2019>
- Seeger, D. R., Golovko, S. A., & Golovko, M. Y. (2020). Blood-brain barrier is the major site for a rapid and dramatic prostanoid increase upon brain global ischemia. *Lipids*, 55, 79–85. <https://doi.org/10.1002/lipid.12205>



- Sharma, V., Dixit, D., Ghosh, S., & Sen, E. (2011). COX-2 regulates the proliferation of glioma stem like cells. *Neurochemistry International*, 59, 567–571.
- Sharp, F. R., & Bernaudin, M. (2004). HIF1 and oxygen sensing in the brain. *Nature Reviews Neuroscience*, 5, 437–448. <https://doi.org/10.1038/nrn1408>
- Sheng, H., Shao, J., Washington, M. K., & DuBois, R. N. (2001). Prostaglandin E₂ increases growth and motility of colorectal carcinoma cells. *Journal of Biological Chemistry*, 276, 18075–18081.
- Simon, M.-P., Tournaire, R., & Pouyssegur, J. (2008). The angiopoietin-2 gene of endothelial cells is up-regulated in hypoxia by a HIF binding site located in its first intron and by the central factors GATA-2 and Ets-1. *Journal of Cellular Physiology*, 217, 809–818. <https://doi.org/10.1002/jcp.21558>
- Spisni, E., Manica, F., & Tomasi, V. (1992). Involvement of prostanoids in the regulation of angiogenesis by polypeptide growth factors. *Prostaglandins Leukotrienes and Essential Fatty Acids*, 47, 111–115. [https://doi.org/10.1016/0952-3278\(92\)90146-A](https://doi.org/10.1016/0952-3278(92)90146-A)
- Stasinopoulos, I., O'Brien, D. R., & Bhujwalla, Z. M. (2009). Inflammation, but not hypoxia, mediated HIF-1 α activation depends on COX-2. *Cancer Biology & Therapy*, 8, 31–35.
- Suresh, K. (2011). An overview of randomization techniques: An unbiased assessment of outcome in clinical research. *Journal of Human Reproductive Sciences*, 4, 8–11. <https://doi.org/10.4103/0974-1208.82352>
- Tarkowski, E., Issa, R., Sjögren, M., Wallin, A., Blennow, K., Tarkowski, A., & Kumar, P. (2002). Increased intrathecal levels of the angiogenic factors VEGF and TGF- β in Alzheimer's disease and vascular dementia. *Neurobiology of Aging*, 23, 237–243.
- Thompson, J. A., Anderson, K. D., DiPietro, J. M., Zwiebel, J. A., Zametta, M., Anderson, W. F., & Maciag, T. (1988). Site-directed neovessel formation in vivo. *Science*, 241, 1349. <https://doi.org/10.1126/science.2457952>
- Toth, P., Rozsa, B., Springo, Z., Doczi, T., & Koller, A. (2011). Isolated human and rat cerebral arteries constrict to increases in flow: Role of 20-HETE and TP receptors. *Journal of Cerebral Blood Flow and Metabolism: Official Journal of the International Society of Cerebral Blood Flow and Metabolism*, 31, 2096–2105.
- Tsuji, M., Kawano, S., Tsuji, S., Sawaoka, H., Hori, M., & DuBois, R. N. (1998). Cyclooxygenase regulates angiogenesis induced by colon cancer cells. *Cell*, 93, 705–716. [https://doi.org/10.1016/S0092-8674\(00\)81433-6](https://doi.org/10.1016/S0092-8674(00)81433-6)
- Tuncer, S., & Banerjee, S. (2015). Eicosanoid pathway in colorectal cancer: Recent updates. *World Journal of Gastroenterology*, 21, 11748–11766. <https://doi.org/10.3748/wjg.v21.i41.11748>
- Verheul, H. M., Panigrahy, D., Yuan, J., & D'Amato, R. J. (1999). Combination oral antiangiogenic therapy with thalidomide and sulindac inhibits tumour growth in rabbits. *British Journal of Cancer*, 79, 114–118. <https://doi.org/10.1038/sj.bjc.6690020>
- Wang, D., & Dubois, R. N. (2010). Eicosanoids and cancer. *Nature Reviews Cancer*, 10, 181–193.
- Wang, D., Wang, H., Guo, Y., Ning, W., Katkuri, S., Wahli, W., Desvergne, B., Dey, S. K., & DuBois, R. N. (2006). Crosstalk between peroxisome proliferator-activated receptor delta and VEGF stimulates cancer progression. *Proceedings of the National Academy of Sciences of the United States of America*, 103, 19069–19074.
- Wang, D., Wang, H., Shi, Q., Katkuri, S., Wahli, W., Desvergne, B., Das, S. K., Dey, S. K., & DuBois, R. N. (2004). Prostaglandin E₂ promotes colorectal adenoma growth via transactivation of the nuclear peroxisome proliferator-activated receptor δ . *Cancer Cell*, 6, 285–295. <https://doi.org/10.1016/j.ccr.2004.08.011>
- Wang, W., Zhu, J., Lyu, F., Panigrahy, D., Ferrara, K. W., Hammock, B., & Zhang, G. (2014). ω -3 polyunsaturated fatty acids-derived lipid metabolites on angiogenesis, inflammation and cancer. *Prostaglandins & Other Lipid Mediators*, 113–115, 13–20. <https://doi.org/10.1016/j.prostaglandins.2014.07.002>
- Ward, N. L., Moore, E., Noon, K., Spassil, N., Keenan, E., Ivanco, T. L., & LaManna, J. C. (2007). Cerebral angiogenic factors, angiogenesis, and physiological response to chronic hypoxia differ among four commonly used mouse strains. *Journal of Applied Physiology*, 102, 1927–1935.
- Wightman, E. L., Haskell-Ramsay, C. F., Thompson, K. G., Blackwell, J. R., Winyard, P. G., Forster, J., Jones, A. M., & Kennedy, D. O. (2015). Dietary nitrate modulates cerebral blood flow parameters and cognitive performance in humans: A double-blind, placebo-controlled, crossover investigation. *Physiology & Behavior*, 149, 149–158. <https://doi.org/10.1016/j.physbeh.2015.05.035>
- Yang, G., Pan, F., Parkhurst, C. N., Grutzendler, J., & Gan, W.-B. (2010). Thinned-skull cranial window technique for long-term imaging of the cortex in live mice. *Nature Protocols*, 5, 201–208. <https://doi.org/10.1038/nprot.2009.222>
- Yanni, S. E., McCollum, G. W., & Penn, J. S. (2010). Genetic deletion of COX-2 diminishes VEGF production in mouse retinal Müller cells. *Experimental Eye Research*, 91, 34–41. <https://doi.org/10.1016/j.exer.2010.03.019>
- Zhang, W., Otsuka, T., Sugo, N., Ardeshiri, A., Alhadid Yazan, K., Iliff Jeffrey, J., DeBarber Andrea, E., Koop Dennis, R., & Alkayed Nabil, J. (2008). Soluble epoxide hydrolase gene deletion is protective against experimental cerebral ischemia. *Stroke*, 39, 2073–2078. <https://doi.org/10.1161/STROKEAHA.107.508325>
- Zhang, Y., & Daaka, Y. (2011). PGE₂ promotes angiogenesis through EP₄ and PKA C γ pathway. *Blood*, 118, 5355–5364. <https://doi.org/10.1182/blood-2011-04-350587>
- Zhang, Z. G., Zhang, L., Jiang, Q., Zhang, R., Davies, K., Powers, C., Bruggen, N. V., & Chopp, M. (2000). VEGF enhances angiogenesis and promotes blood-brain barrier leakage in the ischemic brain. *The Journal of Clinical Investigation*, 106, 829–838. <https://doi.org/10.1172/JCI9369>
- Zhao, L., Wu, Y., Xu, Z., Wang, H., Zhao, Z., Li, Y., Yang, P., & Wei, X. (2012). Involvement of COX-2/PGE₂ signalling in hypoxia-induced angiogenic response in endothelial cells. *Journal of Cellular and Molecular Medicine*, 16, 1840–1855. <https://doi.org/10.1111/j.1582-4934.2011.01479.x>
- Zhong, H., Willard, M., & Simons, J. (2004). NS398 reduces hypoxia-inducible factor (HIF)-1 α and HIF-1 activity: Multiple-level effects involving cyclooxygenase-2 dependent and independent mechanisms. *International Journal of Cancer*, 112, 585–595.
- Zhou, J., Zhang, S., Xue, J., Avery, J., Wu, J., Lind, S. E., & Ding, W.-Q. (2012). Activation of peroxisome proliferator-activated receptor α (PPAR α) suppresses hypoxia-inducible factor-1 α (HIF-1 α) signaling in cancer cells. *The Journal of Biological Chemistry*, 287, 35161–35169. <https://doi.org/10.1074/jbc.M112.367367>
- Zhu, Y., Lee, C., Shen, F., Du, R., Young William, L., & Yang, G.-Y. (2005). Angiopoietin-2 facilitates vascular endothelial growth factor-induced angiogenesis in the mature mouse brain. *Stroke*, 36, 1533–1537. <https://doi.org/10.1161/01.STR.0000170712.46106.2e>

SUPPORTING INFORMATION

Additional supporting information may be found online in the Supporting Information section.

How to cite this article: Seeger DR, Golovko SA, Grove BD, Golovko MY. Cyclooxygenase inhibition attenuates brain angiogenesis and independently decreases mouse survival under hypoxia. *J Neurochem*. 2021;158:246–261. <https://doi.org/10.1111/jnc.15291>